AIR EMISSIONS MEASUREMENTS AT CATTLE FEEDLOTS

by

KRISTEN A. BAUM

B.S., Kansas State University, 2003

A THESIS

submitted in partial fulfillment of the requirements for the degree

MASTER OF SCIENCE

Department of Agronomy
College of Agriculture

KANSAS STATE UNIVERSITY
Manhattan, Kansas

2008

Approved by:

Major Professor
Jay M. Ham

Abstract

The potential environmental impact of animal feeding operations on air quality has created the need for accurate air emissions measurements. Of particular concern are ammonia (NH_3) emissions from cattle feedlots, operations that contribute a large portion of the agricultural NH_3 emissions inventory. Micrometeorological methods are ideal for emissions measurements from large, open-source areas like feedlot pens; however, theoretical assumptions about the boundary layer must be made, which may not hold true above the heterogeneous, fetch-limited surface of the feedlot. Thus, the first objective of this work was to characterize the surface boundary layer of an open-air cattle feedlot and provide insight into how micrometeorological techniques might be applied to these non-ideal sites. Eddy covariance was used to measure fluxes of momentum, heat, water, and carbon dioxide from a commercial cattle feedlot in central Kansas. Data supported the use of eddy covariance and similar methods (i.e., relaxed eddy accumulation) for flux measurements from both cattle and pen surfaces. The modeled cumulative source area contributing to eddy covariance measurements at a 6-m sample height was dominated by just a few pens near the tower, making the characteristics of those pens especially important when interpreting results. The second objective was to develop a system for measuring NH_3 fluxes from feedlots. A new type of relaxed eddy accumulation system was designed, fabricated, and tested that used honeycomb denuders to independently sample NH_3 in up- and down-moving eddies. Field testing of the relaxed eddy accumulation system at a feedlot near Manhattan, KS showed fluxes of NH_3 ranged between 60 and 130 $\mu g\ m^{-2}\ s^{-1}$ during the summer of 2007. Even in the high NH_3 environment (e.g., 300-600 $\mu g\ m^{-3}$), the honeycomb denuders had enough capacity for the 4-hour sampling duration and could be used to measure other chemical species that the denuders could be configured to capture. Results provide a foundation for emissions measurements of NH_3 and other gases at cattle feedlots and help address some of the challenges that micrometeorologists face with any non-ideal source area.

Table of Contents

List of Figures

List of Tables

List of Symbols

$C_x(f)$		power cospectra
D		Hsieh et al., (2000) footprint model constant
λE	($W\ m^{-2}$)	latent heat flux
F	($kg\ m^{-2}\ s^{-1}$)	mass flux
F_c	($mg\ m^{-2}\ s^{-1}$)	CO_2 flux
F_{pen}	($g\ m^{-2}\ s^{-1}$)	flux per unit pen area
F_{raw}	($g\ m^{-2}\ s^{-1}$)	total flux
H	($W\ m^{-2}$)	sensible heat flux
L	(m)	Obukhov length
P		Hsieh et al., (2000) footprint model constant
S	(m^2)	surface area
S_{pens}		fraction of weighted source area attributed to pens
S_{total}		total weighted source area
$S_x(f)$		power spectra
T	(C)	temperature
X_f	(m)	Hsieh modeled upwind distance representing a fraction, f, of the source area
b	(m)	breadth of roughness elements
d	(m)	displacement height
db	($m\ s^{-1}$)	deadband
f	(Hz)	frequency
$f_{u/d}$	(kg dry air s^{-1})	continuous flowrates through up/down-moving eddy traps
h	(m)	height of roughness elements
k		von Karman's constant, 0.41
$m_{u/d}$	(mg)	mass from up/down-moving eddies
n		number of roughness elements
s		scalar of interest
t	(s)	total sample duration

u	($m\ s^{-1}$)	horizontal wind speed
u_z	($m\ s^{-1}$)	horizontal wind speed at measurement height, z
u^*	($m\ s^{-1}$)	friction velocity
w	($m\ s^{-1}$)	vertical wind speed
x	(m)	horizontal distance from measurement location
z	(m)	measurement height
z_u	(m)	Hsieh et al., (2000) footprint model length scale
z_0	(m)	roughness length
A		frontal area index
Δ_{ITT}	(%)	integral turbulence test
Δ_{ST}	(%)	stationarity test
Λ		canopy area index
Ψ_m		diabatic correction factor for momentum
$\alpha_{u/d}$		fraction of time up/down-moving eddy valves are activated
β		relaxation factor
λ	($J\ g^{-1}$)	latent heat of vaporization of water
ρ	($kg\ m^{-3}$)	air density
ρ_d	($kg\ m^{-3}$)	dry air density
σ_w	($m\ s^{-1}$)	standard deviation of the vertical wind speed
ϕ_w		similarity function for vertical wind speed
$\chi^{+/-}$	($kg\ kg^{-1}$)	mixing ratio of up/down-moving eddies

Acknowledgements

I would like to acknowledge the USDA Cooperative State Research, Education and Extension Service Air Quality Program, National Research Initiative and the Department of Agronomy for financial support. I would like to acknowledge Fred Caldwell, Jamey Duesterhaus, Kira Arnold, and many undergraduate student workers for their technical support. I would like to acknowledge Patrick Coyne and Spencer Casey at the Agricultural Research Center at Hays for providing survey-grade mapping and GIS analysis for one of the feedlot study sites. I would like to acknowledge Nathanial Brunsell at the University of Kansas for his help with the spectral analysis. I would like to acknowledge my committee members, Gary Pierzynski and Ronaldo Maghirang, and especially my major professor, Jay Ham for their guidance with this work. Finally, I would like to acknowledge my family, friends, and my husband, Shane, for all their support and encouragement.

CHAPTER 1 - Introduction

A recent report by the Food and Agriculture Organization of the United Nations estimates that the livestock industry's contribution of global anthropogenic emissions is about 9% for carbon dioxide (CO_2), 35-40% for methane (CH_4), 65% for nitrous oxide (N_2O) and 64% for ammonia (NH_3) (Steinfeld et al., 2006). With increasing interest in the livestock industry's impact on air quality, there is a need for more accurate inventories of gaseous and particulate emissions from animal feeding operations, dictating the need for more emissions measurements from different types of livestock production, under a range of management systems, and at multiple geographical locations (National Research Council, 2003).

In 1999, the United States Environmental Protection Agency (USEPA) established regulations regarding regional haze, the impairment of visibility due to pollutant emissions from a variety of sources covering a wide geographic area, with a specific focus on improved visibility for Class I areas (i.e., national parks and wilderness areas) (USEPA, 1999). These regulations prompted the EPA to include NH_3 in the consolidated emission inventory reporting requirements because NH_3 is a precursor to $PM_{2.5}$, a major contributor to regional haze (USEPA, 2002). Additionally, researchers have shown that NH_3 deposition can lead to soil acidification (ApSimon et al., 1987; Brunet et al., 1998) and shifts in species composition (Bobbink et al., 1998; Pittcairn et al., 1998). Because the livestock industry is such a large component of anthropogenic NH_3 emissions, accurate estimates of emissions from these sources are crucial.

According to the 2002 Census of Agriculture, almost half of the market value of the US livestock industry came from cattle (NASS, 2004a). Nearly 30 million cattle on feed are marketed from feedlots every year, with around 60% coming from operations with a capacity greater than 16,000 head (NASS, 2004b). In the US, these large-scale feedlots are typically open-air, earthen surface lots, with over 80% located in the high plains states of Texas, Oklahoma, Kansas, Nebraska, and Colorado (NASS, 2004b). Incidentally, some of these feedlots are located within the same geographic vicinity as Class I areas, so emissions measurements from these feedlots are especially important.

Quantifying emissions from feedlots has proven to be challenging. Various techniques have been applied including mass balances, chambers, tracer ratio methods, dispersion modeling, and micrometeorological methods. While many of these methods have shown promise, virtually all of them remain largely untested in feedlot situations.

A few studies have used the mass balance approach for quantifying total N emissions by estimating N lost as the difference between all N additions and subtractions, which included cattle intake and retention, manure removal via pen cleaning, pen surface retention, and runoff (Adams et al., 2004; Bierman et al., 1999; Erickson and Klopfenstein 2001a, b; Farran et al., 2006). While this method is straight forward and has the advantage of conservation of mass, different N species are not distinguished (e.g., N_2O vs. NH_3 vs. NH_4^+).

Various chamber techniques have been used to measure a number of emissions from either feedlot surfaces (Boadi et al., 2004; Ellis et al., 2001; Misselbrook et al., 2001, 2006) or feedlot cattle (Beauchemin and McGinn, 2005, 2006; McGinn et al., 2004, 2006a). While chambers are quite useful for surfaces with uniform emissions, such as fields with land-applied animal waste, the heterogeneity of the feedlot surface is problematic. In the case of whole animal chambers, stress and reduced mobility of the animals may reduce intake (McGinn et al., 2004), likely altering emissions. Finally, another drawback of any chamber technique is that the environment is modified, impacting emissions as well.

Tracer ratio methods have traditionally been used to quantify CH_4 emissions from individual cattle (Boadi et al., 2002a, b, 2004; Boadi and Wittenberg, 2002; Johnson et al., 1994; Lassey et al., 1997; McCaughey et al., 1997; McGinn et al., 2006a; Pinares-Patino et al., 2003), but Kaharabata et al. (2000) applied a technique developed for natural gas facilities (Lamb et al., 1995) to a dairy cow feedlot. This method is simple in that it only requires that a tracer gas be emitted at a known rate near the CH_4 source and the concentrations of CH_4 and the tracer gas be measured downwind. However, it relies heavily on the assumption that the tracer emissions are representative of the CH_4 emissions (i.e., sources/sinks are the same) and are transported by the same turbulent eddies.

Flesch et al. (2007) and McGinn et al. (2006b, 2007) applied an inverse dispersion technique at feedlots to estimate NH_3 and CH_4 emissions, where a single, line-averaged concentration was measured at a downwind distance and a backward Lagrangian stochastic dispersion model was used to infer the emission rate of the source. In a previous study this technique was applied to a simulated feedlot with known CH_4 emissions and in spite of the surface complexity, emissions could be predicted to within 2%, depending on where the concentration was measured and whether ambient or in-plot wind statistics were used (Flesch et al., 2005). As with any approach that involves modeling turbulent transport, accuracy of the results depends on the accuracy of both the model and model inputs. Although these methods have shown promise and improved our understanding of feedlot emissions, they remain largely untested.

Micrometeorological methods (e.g., eddy covariance, relaxed eddy accumulation) are often considered the best methods for measuring fluxes from CAFOs (Shah et al., 2006) and would be ideal in feedlot situations because they provide areally averaged flux measurements for large areas without disturbing the surface. The micrometeorological gradient method has already been used in a few feedlot studies (Hutchinson et al., 1982; Harper et al., 1999; Baek et al., 2006; Todd et al., 2007). However, gradient methods rely on strict assumptions including steady-state conditions, horizontally homogenous sources and sinks of flux, and conformity to Monin-Obukhov similarity theory (Prueger and Kustas, 2005). Single-height flux measurements such as eddy covariance, while still requiring certain assumptions, might be more appropriate when patchiness in the footprint is an issue. Regardless of the micrometeorological technique employed, unique characteristics of cattle feedlots, namely the various scales of surface heterogeneity and strong emissions of certain gases from the animals (i.e., moving and sometimes clustered point sources of gas) present a challenge. Assumptions underlying various micrometeorological measurement techniques might not hold true at feedlots when measuring specific compounds under certain circumstances. In these situations, fundamental knowledge of the surface boundary layer is needed to determine whether micrometeorological methods can be applied with confidence to these non-ideal, fetch-limited surfaces.

Consequently, the first goal of this study was to characterize the surface boundary layer of an open-air cattle feedlot. Specifically, objectives were to: (1) determine the orthogonal distributions of wind speed and atmospheric stability; (2) calculate the roughness length and displacement height; (3) perform a spectral analysis of turbulence above the pens; (4) determine required sampling frequencies (e.g., 10 or 20 Hz) and integration intervals for flux calculations (i.e., ogive analysis); (5) develop composite curves of diurnal CO_2, latent heat, and sensible heat fluxes; (6) determine fetch requirements; (7) map the feedlot and determine the fraction of the surface covered by pens, roads, alleys, etc.; and (8) evaluate the source area footprint to account for the diluting effect of roads and other non-pen surfaces.

The second goal of this work was to develop a technology for measuring NH_3 emissions at cattle feedlots using relaxed eddy accumulation (REA). The objective was to adapt the Chemcomb Speciation Sampling Cartridge (model 3500, Thermo Scientific, Waltham, MA) to a REA system for the measurement of NH_3 gases and NH_4^+ aerosol fluxes at cattle feedlots. A new type of REA system was designed, fabricated, and tested. This system utilized honeycomb denuders that independently sampled NH_3 in up- and down-moving eddies. This system was designed specifically for measuring NH_3 fluxes in high NH_3 environments, but could be applied to measure anything that the denuders and/or filterpacks can be configured to capture.

This work provides guidance on the use of eddy covariance and other micrometeorological techniques for measuring gaseous and aerosol emissions at cattle feedlots. Results also provide a foundation for emissions measurements of NH_3 and other gases at cattle feedlots and helps address some of the challenges that micrometeorologists face with any non-ideal source area.

References

Adams, J.R., Farran, T.B., Erickson, G.E., Klopfenstein, T.J., Macken, C.N., Wilson, C.B., 2004. Effect of organic matter addition to the pen surface and pen cleaning frequency on nitrogen mass balance in open feedlots. J. Anim. Sci. 82, 2153-2167.

ApSimon, H.M., Kruse, M., Bell, J.N.B., 1987. Ammonia emissions and their role in acid deposition. Atmos. Environ. 21, 1939-1946.

Baek, B.-H., Todd, R., Cole, N.A., Koziel, J.A., 2006. Ammonia and hydrogen sulphide flux and dry deposition velocity estimates using vertical gradient method at a commercial beef cattle feedlot. Int. J. Global Env. Issues 6(2/3), 189-203.

Beauchemin, K.A., McGinn, S.M., 2005. Methane emissions from feedlot cattle fed barley or corn diets. J. Anim. Sci. 83, 653-661.

Beauchemin, K.A., McGinn, S.M., 2006. Methane emissions from beef cattle: effects of fumaric acid, essential oil, and canola oil. J. Anim. Sci. 84, 1489-1496.

Bierman, S., Erickson, G.E., Klopfenstein, T.J., Stock, R.A., Shain, D.H., 1999. Evaluation of nitrogen and organic matter balance in the feedlot as affected by level and source of dietary fiber. J. Anim. Sci. 77, 1645-1653.

Boadi, D.A., Wittenberg, K.A., 2002. Methane production from dairy and beef heifers fed forages differing in nutrient density using the sufphur hexafluoride (SF_6) tracer gas technique. Can J. Anim. Sci. 82, 201-206.

Boadi, D.A., Wittenberg, K.M., Kennedy, A.D., 2002a. Validation of the sulphur hexafluoride (SF_6) tracer gas technique for measurement of methane and carbon dioxide production by cattle. Can. J. Anim. Sci. 82, 125-131.

Boadi, D.A., Wittenberg, K.M., McCaughey, W.P., 2002b. Effects of grain supplementation on methane production of grazing steers using the sulphur (SF_6) tracer gas technique. Can. J. Anim. Sci. 82, 151-157.

Boadi, D.A., Wittenberg, K.M., Scott, S.L., Burton, D., Buckley, K., Small, J.A., Ominski, K.H., 2004. Effect of low and high forage diet on enteric and manure pack greenhouse gas emissions from a feedlot. Can. J. Anim. Sci. 84, 445-453.

Bobbink, R., Hornung, M., Roelofs, J.G.M., 1998. The effects of air-borne nitrogen pollutants on species diversity in natural and semi-natural European vegetation. J. Ecol. 86, 717-738.

Brunet, J., Diekmann, M., Falkengren-Grerup, U., 1998. Effects of nitrogen deposition on field layer vegetation in south Swedish oak forests. Environ. Pollut. 102(SI), 35-40.

Ellis, S., Webb, J., Misselbrook, T., Chadwick, D., 2001. Emission of ammonia (NH_3), nitrous oxide (N_2O) and methane (CH_4) from a dairy hardstanding in the UK. Nut. Cyc. Agroecosys. 60, 115-122.

Erickson, G.E., Klopfenstein, T.J., 2001a. Managing N inputs and the effect on N losses following excretion in open-dirt feedlots in Nebraska. *In* Optimizing Nitrogen Management in Food and Energy Production and Environmental Protection: Proceedings of the 2nd International Nitrogen Conference on Science and Policy. TheScientificWorld 1(S2), 830-835.

Erickson, G.E., Klopfenstein, T.J., 2001b. Nutritional methods to decrease N losses from open-dirt feedlots in Nebraska. *In* Optimizing Nitrogen Management in Food and Energy Production and Environmental Protection: Proceedings of the 2nd International Nitrogen Conference on Science and Policy. TheScientificWorld 1(S2), 836-843.

Farran, T.B., Erickson, G.E., Klopfenstein, T.J., Macken, C.N., Lindquist, R.U., 2006. Wet corn gluten feed and alfalfa hay levels in dry-rolled corn finishing diets: effects on finishing performance and feedlot nitrogen mass balance. J. Anim. Sci. 84, 1205-1214.

Flesch, T.K., Wilson, J.D., Harper, L.A., 2005. Deducing ground-to-air emissions from observed trace gas concentrations: a field trial with wind disturbance. J. App. Meteorol. 44, 475-484.

Flesch, T.K., Wilson, J.D., Harper, L.A., Todd, R.W., Cole, N.A., 2007. Determining ammonia emissions from a cattle feedlot with an inverse dispersion technique. Agric. For. Meteorol. 144, 139-155.

Harper, L.A., Denmead, O.T., Freney, J.R., Byers, F.M., 1999. Direct measurements of methane emissions from grazing and feedlot cattle. J. Anim. Sci. 77, 1392-1401.

Hutchinson, G.L., Mosier, A.R., Andre, C.E., 1982. Ammonia and amine emissions from a large cattle feedlot. J. Env. Qual. 11(2), 288-293.

Johnson, K., Huyler, M., Westberg, H., Lamb, B., Zimmerman, P., 1994. Measurement of methane emissions from ruminant livestock using a SF_6 tracer technique. Env. Sci. Tech. 28(2), 359-362.

Kaharabata, S.K., Schuepp, P.H., Desjardins, R.L., 2000. Estimating methane emissions from dairy cattle housed in a barn and feedlot using an atmospheric tracer. Env. Sci. Tech. 34, 3296-3302.

Lamb, B.K., McManus, J.B., Shorter, J.H., Kolb, C.E., Mosher, B., Harriss, R.C., Allwine, E., Blaha, D., Howard, T., Guenther, A., Lott, R.A., Siverson, R., Westberg, H., Zimmerman, P., 1995. Development of atmospheric tracer methods to measure methane emissions from natural gas facilities and urban areas. Env. Sci. Tech. 29, 1468-1479.

Lassey, K.R., Ulyatt, M.J., Martin, R.J., Walker, C.F., Shelton, I.D., 1997. Methane emissions measured directly from grazing livestock in New Zealand. Atmos. Env. 31, 2905-2914.

McCaughey, W.P., Wittenberg, K., Corrigan, D., 1997. Methane production by steers on pasture. Can. J. Anim. Sci. 77, 519-524.

McGinn, S.M., Beauchemin, K.A., Coates, T., Colombatto, D., 2004. Methane emissions from beef cattle: effects of monensin, sunflower oil, enzymes, yeast, and fumaric acid. J. Anim. Sci. 82, 3346-3356.

McGinn, S.M., Beauchemin, K.A., Iwaasa, A.D., McAllister, T.A., 2006a. Assessement of the sulfur hexafluoride (SF_6) tracer technique for measuring enteric methane emissions from cattle. J. Env. Qual. 35, 1686-1691.

McGinn, S.M., Flesch, T.K., Harper, L.A., Beauchemin, K.A., 2006b. An approach for measuring methane emissions from whole farms. J. Env. Qual. 35, 14-20.

McGinn, S.M., Flesch, T.K., Crenna, B.P., Beauchemin, K.A., Coates, T., 2007. Quantifying ammonia emissions from cattle feedlot using a dispersion model. J. Environ. Qual. 36, 1585-1590.

Misselbrook, T.H., Webb, J., Chadwick, D.R., Ellis, S., Pain, B.F., 2001. Gaseous emissions from outdoor concrete yards used by livestock. Atmos. Env. 35, 5331-5338.

Misselbrook, T.H., Webb, J., Gilhespy, S.L., 2006. Ammonia emissions from outdoor concrete yards used by livestock—quantification and mitigation. Atmos. Env. 40, 6752-6763.

National Agricultural Statistics Service, United States Department of Agriculture. 2004a. 2002 census of agriculture: U.S. national level data. United States Government Printing Office. Washington D.C. http://www.nass.usda.gov/census/census02/volume1/us/index1.htm

National Agricultural Statistics Service, United States Department of Agriculture. 2004b. Cattle: final estimates 1999-2003. United States Government Printing Office. Washington D.C. http://usda.mannlib.cornell.edu/usda/nass/SB989/sb989.pdf

National Research Council. 2003. Air emissions from animal feeding operations: current knowledge, future needs. The National Academies Press. Washington D.C.

Pinares-Patino, C.S., Baumont, R., Martin, C., 2003. Methane emissions by Charolais cows grazing a monospecific pasture of timothy at four stages of maturity. Can. J. Anim. Sci. 83, 769-777.

Pittcairn, C.E.R., Lieth, I.D., Sheppard, L.J., Sutton, M.A., Fowler, D., Munro, R.C., Tang, S., Wilson, D., 1998. The relationship between nitrogen deposition, species composition and foliar nitrogen concentrations in woodland flora in the vicinity of livestock farms. Environ. Pollut. 102(1/1), 41-48.

Prueger, J.H., Kustas., W.P., 2005. Aerodynamic principles of flux-profile relationships. In *Micrometeorology in agricultural systems*, Madison, WI. Agronomy Monograph 47, ASA, CSSA, SSSA.

Shah, S.B., Westerman, P.W., Arogo, J., 2006. Measuring ammonia concentrations and emissions from agricultural land and liquid surfaces: a review. J. of Air and Waste Management Association. 56, 945-960.

Steinfeld, H., Gerber, P., Wassenaar, T., Castel, V., Rosales, M., de Haan, C., 2006. Livestock's Long Shadow: Environmental Issues and Options. Food and Agriculture Organization of the United Nations.

Todd, R.W., Cole, N.A., Harper, L.A., Flesch, T.K., 2007. Flux-gradient estimates of ammonia emissions from beef cattle feedyard pens. *In* Proceedings of the ASABE International Symposium on Air Quality and Waste Management for Agriculture, September 16-19, 2007, Broomfield, Colorado. CD-ROM.

United States Environmental Protection Agency. 1999. Regional haze regulations; final rule. Fed. Register 64(126), 35714-35774.

United States Environmental Protection Agency. 2002. Consolidated emissions reporting; final rule. Fed. Register 67(111), 39602-39616.

CHAPTER 2 - Surface Boundary Layer of Cattle Feedlots: Implications for Air Emissions Measurement

2.1 Introduction

Confined animal feeding operations (CAFOs) can affect air quality at local, regional, and global scales through emissions of trace gases (e.g., NH_3, N_2O, CH_4, VOCs), particulates ($PM_{2.5}$, PM_{10}), and odors. However, field measurements are limited, and there is a need for more accurate quantification of gaseous and particulate emissions from different types of CAFOs in the United States (National Research Council, 2003; Steinfeld et al., 2006). Few studies have attempted to quantify emissions from open-air, earthen-surface cattle feedlots in the United States (Casey et al., 2006). Nearly 30 million cattle on feed are marketed from these feedlots every year, with around 60% coming from large-scale operations (capacity greater than 16,000 head), more than 80% of which are located in the High Plains states of Texas, Oklahoma, Kansas, Nebraska, and Colorado (National Agricultural Statistics Service, 2004). More than 9 million cattle are held at feedlots in this region throughout the year, and the feed nitrogen (N) for these animals, 0.23 kg animal^{-1} d^{-1} (Kissinger et al., 2007), totals more than 2 million kg of N per day. Preliminary estimates suggest up to 50% of feed N is lost to the atmosphere (Flesch et al., 2007; Cole et al., 2007). Thus, emissions of ammonia (NH_3-N) from feedlots in the High Plains could be more than 2 million kg per day or 0.38 Tg annually—about 12% of total United States emissions (van Aardenne et al., 2001). Clearly, gaseous losses from feedlots are an important component of the anthropogenic emissions inventory. Data are needed to better understand the feedlot boundary layer and improve measurement and modeling of emissions from these CAFOs.

Quantifying emissions from cattle feedlots is challenging. A few studies have used the mass balance approach for quantifying total feedlot N emissions, but this method cannot distinguish between N species (e.g., N_2O vs. NH_3) (Adams et al., 2004; Bierman et al., 1999; Erickson and Klopfenstein, 2001a, b; Farran et al., 2006). Kaharabata et al.

(2000) applied a tracer ratio technique developed for natural gas facilities (Lamb et al., 1995) to estimate methane (CH_4) emissions from a dairy cow feedlot, but its accuracy depends on the tracer gas emissions being representative of the CH_4 emissions. Various chamber techniques have been used to measure a number of emissions from either feedlot surfaces (Boadi et al. 2004; Ellis et al. 2001; Misselbrook et al., 2001, 2006) or feedlot cattle (Beauchemin and McGinn, 2005; 2006; McGinn et al., 2004, 2006a), but these techniques alter the environment and can be unrepresentative of natural conditions (Cole et al., 2007). Flesch et al. (2007) and McGinn et al. (2006b, 2007) applied inverse dispersion techniques at feedlots to estimate NH_3 and CH_4 emissions using a backward Lagrangian stochastic dispersion model. As with any approach that involves modeling turbulent transport, accuracy of the results depends on the accuracy of both the model and model inputs. Although these methods have shown promise and improved our understanding of feedlot emissions, they remain largely untested.

Micrometeorological methods (e.g., eddy covariance, relaxed eddy accumulation) are often considered the best methods for measuring fluxes from CAFOs (Shah et al., 2006) and would be ideal in feedlot situations because they provide areally averaged flux measurements for large areas without disturbing the surface. The micrometeorological gradient method has already been used in a few feedlot studies (Hutchinson et al., 1982; Harper et al., 1999; Baek et al., 2006; Todd et al., 2007). However, gradient methods rely on strict assumptions including steady-state conditions, horizontally homogenous sources and sinks of flux, and conformity to Monin-Obukhov similarity theory (Prueger and Kustas, 2005). Single-height flux measurements such as eddy covariance, while still requiring certain assumptions, might be more appropriate when patchiness in the footprint is an issue. Regardless of the micrometeorological technique employed, unique characteristics of cattle feedlots, namely the various scales of surface heterogeneity and strong emissions of certain gases from the animals (i.e., moving and sometimes clustered point sources of gas) present a challenge. Assumptions underlying various micrometeorological measurement techniques might not hold true at feedlots when measuring specific compounds under certain circumstances. In these situations, fundamental knowledge of the surface boundary layer is needed to determine whether

micrometeorological methods can be applied with confidence to these non-ideal, fetch-limited surfaces.

The goal of this study was to characterize the surface boundary layer of an open-air cattle feedlot. Specifically, objectives were to: (1) determine the orthogonal distributions of wind speed and atmospheric stability; (2) calculate the roughness length and displacement height; (3) perform a spectral analysis of turbulence above the pens; (4) determine required sampling frequencies (e.g., 10 or 20 Hz) and integration intervals for flux calculations (i.e., ogive analysis); (5) develop composite curves of diurnal CO_2, latent heat, and sensible heat fluxes; (6) determine fetch requirements; (7) map the feedlot and determine the fraction of the surface covered by pens, roads, alleys, etc.; and (8) evaluate the source area footprint to account for the diluting effect of roads and other non-pen surfaces. These assessments provide some guidance on the use of eddy covariance and other micrometeorological techniques for measuring gaseous and aerosol emissions at cattle feedlots.

2.2 Methods and Materials

Research was conducted at a commercial cattle feedlot in western Kansas that has been in operation for more than 25 years. The area receives around 570 mm of precipitation annually and has an average annual temperature of about 12.5°C. The terrain is level to gently sloping with slopes less than 5%, and the soils are loamy fine sands and fine sandy loams. The feedlot has a one-time capacity of approximately 30,000 animals, with pens covering roughly 62 ha. Cattle enter the feedlot weighing an average of 300 to 350 kg. They are fed a high-concentrate finishing diet for around 180 days and leave the feedlot weighing an average of 550 to 600 kg. Stocking densities range from 15 to 18 m^2 $animal^{-1}$. Pens are scraped and manure is removed annually. Feedlot pens, roads, and other structures were measured with a survey grade RTK GPS rover and base station system (AgGPS 214, Trimble Navigation Limited, Sunnyvale, CA) and mapped using ArcGIS 9.0 software (ESRI, Redlands, CA). Feedlot layout is shown in Figure 2.1.

Fluxes of sensible heat (H), latent heat (λE), and CO_2 (F_c) were measured with an eddy covariance (EC) system consisting of a 3D sonic anemometer (CSAT3, Campbell

Scientific, Inc., Logan, UT) and an open-path infrared gas analyzer (LI-7500, LI-COR Biosciences, Lincoln, NE). These systems also provided component wind vectors (u, v, and w) and scalar measurements of temperature (T), water vapor (H_2O) concentration, CO_2 concentration, and atmospheric pressure. Data were collected from July 2006 through April 2007. The EC system was deployed at 6 m above the pen surface along the northern edge of the pens, resulting in about 1600 m of fetch when winds were from the predominant southerly direction (Figure 2.1). Eddy covariance signals were sampled and stored at 20 Hz with a CR1000 datalogger (Campbell Scientific, Inc.) equipped with a CFM100 card reader. The open-path gas analyzer was calibrated monthly using tank gas and a dew point generator (LI-610, LI-COR Biosciences).

All high-frequency EC data were post-processed with the EdiRe software package (version 1.4.3.1167, R. Clement, University of Edinburgh, UK) closely following the guidelines described in Lee et al. (2004). Eddy covariance fluxes were subject to the following corrections: despiking, planar fit coordinate rotation, lag removal, sonic-temperature sensible heat flux corrections, density corrections for CO_2 and H_2O, and frequency response corrections. Other calculations performed with EdiRe included calculation of friction velocity, u_* (m s^{-1}); stability parameter, z/L, where L is the Obukhov length (m); and stationarity tests. MATLAB (version 7.2.0.232, The Mathworks, Inc., Natick, MA) was used for any remaining calculations or post-processing.

Periods with questionable data were excluded using quality control filters similar to those described by Hammerle et al. (2007), which included stationarity and integral turbulence tests (Foken and Wichura, 1996) and a footprint test. For the stationarity test, 30-min covariances between the vertical wind speed (w) and both the horizontal wind speed (u) and scalars (T, H_2O, CO_2) were compared with the average of six consecutive 5-min covariances for the same period. Periods where deviations, Δ_{ST}, were greater than 30% for any of the four were considered unstationary and were excluded from analysis:

$$\Delta_{ST} = \frac{100\left|\overline{w's'_5} - w's'_{30}\right|}{w's'_{30}} \tag{2.1}$$

where s is the scalar of interest, and 5 and 30 are subscripts for the 5- and 30-min covariances. For the integral turbulence test (ITT), the deviation from Monin-Obukhov

theory was determined by comparing the similarity function for vertical wind speed, ϕ_w, representing the ratio of the standard deviation of w (σ_w) and u_*, with modeled functions developed by Kaimal and Finnigan (1994):

$$\phi_w = \frac{\sigma_w}{u_*} = \begin{cases} 1.25\left(1+3\left|z/L\right|\right)^{1/3}, & -2 \le z/L < 0 \\ 1.25\left(1+0.2\,z/L\right), & 0 \le z/L < 1 \end{cases} \tag{2.2}$$

where L is the Obukhov length (m) and z is measurement height (m). Any periods where the percent deviation between the observed and modeled similarity functions, Δ_{ITT}, was greater than 30% were excluded from analysis:

$$\Delta_{ITT} = \frac{100\left|\frac{\sigma_w}{u_*} - \phi_w\right|}{\phi_w} \tag{2.3}$$

For the footprint test, an approximate analytical footprint model developed by Hsieh et al. (2000) was used to calculate the distance upwind from the measurement location, X_f (m), representing a fraction (f) of the source area of the flux measurement:

$$X_f = \frac{-D\left|L\right|^{(1-P)} z_u^P}{k^2 \ln(f)} \tag{2.4}$$

with

$$z_u = z\left(\ln(z/z_0) - 1 + z_0/z\right) \tag{2.5}$$

where z_0 is the roughness length (m), k is von Karman's constant, and

D = 0.28, P = 0.59 for unstable conditions

D = 0.97, P = 1.00 for neutral conditions (|z/L| < 0.02), and

D = 2.44, P = 1.33 for stable conditions.

Periods were excluded when the length of the footprint, X_f, computed using f = 70%, extended beyond the boundary of the feedlot (i.e., pens). The rationale for using $X_{70\%}$ as the fetch requirement is discussed in Section 2.3.4 Determining Fetch Requirements.

Roughness lengths were calculated for each 30-min period by rearranging the wind profile equation as follows:

$$z_0 = \frac{z-d}{\exp\left(\frac{ku_z}{u_*} + \Psi_m\right)} \tag{2.6}$$

where d is the displacement height (m), u_z is the windspeed at the measurement height (m s^{-1}), and Ψ_m is the diabatic correction factor for momentum computed from the Obukhov length following the approach of Businger et al. (1971) and Dyer (1974).

Because cattle act like bluff-rough elements on the surface, d was determined using a simplified empirical model developed by Raupach (1994) that is designed for sparse canopies (i.e., sparse shrublands, desert). The model is based on a physical parameter called the frontal area index, A, defined as the frontal area of roughness elements per unit ground area:

$$A = nbh/S \tag{2.7}$$

where b is the roughness element breadth (m), h is the roughness element height (m), n is the total number of roughness elements, and S is the total surface area (m^2). This model is especially well-suited for the feedlots, where cattle size and density per pen are known. Using the average weight of the cattle at the site (440 kg), b and h were estimated as 1.08 and 1.20 m, respectively, with regression equations developed by the American Society of Agricultural and Biological Engineers (ASABE, 2006). Displacement height was then calculated using best-fit coefficients for d found by Verhoef et al. (1997b), who compared modeled estimates of d with experimentally determined values of d from a variety of sparse canopies:

$$d = h - \frac{h\left(1 - \exp\left(-\sqrt{42\Lambda}\right)\right)}{\sqrt{42\Lambda}} \tag{2.8}$$

where Λ is the canopy area index, $\Lambda = 2A$.

The majority of CO_2 emissions from feedlots originate from cattle respiration and ruminant digestion. The animals are essentially an arrangement of mobile bluff bodies and point sources of CO_2 – sometimes clustered and sometimes distributed more uniformly in the pen. In contrast, sensible heat fluxes arise primarily from the pen surface, an areal source. Thus, it is possible that the EC system might attenuate turbulent signals of the CO_2 and T differently, especially at high and low frequencies. To evaluate performance of the EC system in the frequency domain, the power spectra, $S_x(f)$, for CO_2 and T, and the cospectra, $C_x(f)$, of these scalars with vertical wind speed (w) were calculated from 20-Hz time series. Processing techniques were similar to those used by Blanken et al. (1998). Analyses are shown for eight 30-min segments collected between

1000 and 1400 LST on August 30, 2006, which was a typical summer day at the feedlot. Data from each 30-min segment were linearly detrended and the spectra and cospectra computed using Welch's method in MATLAB (Mathworks Inc.). Values of S_x and C_x were normalized by the variance of x and covariance of x and w, respectively, and plotted with respect to normalized frequency, $f \cdot z_m/u$, where z_m was measurement height less d and u was the mean horizontal wind speed. To avoid cluttering the log-log plots with too many points, S_x and C_x were bin-averaged for 50 equally spaced intervals on the x-axis (i.e., log $f \cdot z_m/u$).

Cospectral analyses were also used to determine how much of the total flux could be attributed to frequencies greater than 1 Hz in order to establish the minimum sampling rate that would keep uncertainty around the flux estimate low. The integral of the complete 20-Hz-derived co-spectrum was compared with integrals that progressively omitted sections of the higher frequency cospectra. Ogive functions were computed to determine if low frequency transport processes (i.e., those with periods greater than 30 min) were affecting the eddy flux calculations (Moncrieff et al., 2004). Periods out to 2.0 hours were evaluated to test for the effect of eddies of increasing larger periods.

Composite curves were developed for diurnal F_c, λE, and H by averaging measurements of flux based on the time of day using only those periods where it could be assumed with reasonable confidence that fluxes originated within pen boundaries. Periods included in the calculations had at least a 100:1 fetch to height ratio (wind direction between 155 and 190 degrees) and atmospheric stability that was classified as either neutral or unstable. In this case, the cutoff for the stationarity filter was increased from 30% to 60% to include more data in the averages while still retaining periods of at least acceptable quality (Foken et al., 2004).

Hsieh et al. (2000) footprint modeling was also used to examine the cumulative source area footprint for six months of measurements (i.e., the feedlot pen layout was overlaid with an EC source area map). The one-dimensional flux density distribution is calculated as a function of upwind distance (x) and L:

$$f(x,z_0) = \frac{1}{k^2 x^2} D z_u^P |L|^{1-P} \exp\left(\frac{-1}{k^2 x} D z_u^P |L|^{1-P}\right) \tag{2.9}$$

For each 30-min period, flux densities were calculated over 10-m intervals upwind of the measurement location by integrating the modeled flux density distribution:

$$\int_{x-2}^{x+2} f(x,z_0) = \exp\left(\frac{-1}{k^2(x+5)} D z_u^P |L|^{1-P}\right) - \exp\left(\frac{-1}{k^2(x-5)} D z_u^P |L|^{1-P}\right) \qquad (2.10)$$

A 1° by 4-m polar grid was created with the measurement location as the origin. The 30-min periods were sorted based on wind direction, and the integrated flux densities for each grid location were summed, resulting in a grid of x-y locations and corresponding cumulative flux densities.

Carbon dioxide, and to a lesser extent H_2O fluxes, from the roads and alleys were likely very low compared with those from the pens, especially when the surface was dry. Thus, raw fluxes were scaled upward to estimate flux per unit pen area and, ultimately, flux per unit animal. The Hsieh model was run for each 30-min period and mathematically projected over the feedlot map based on wind direction. Total flux was assumed to originate with $X_{70\%}$ as discussed in 2.3.4 Determining Fetch Requirements. The fraction of the weighted source area, S, that was attributed to pen surface could be determined. After assuming negligible flux from the non-pen surfaces, the flux per unit pen area, F_{pen}, was calculated as:

$$F_{pen} = F_{raw}\left(\frac{S_{total}}{S_{pens}}\right) \qquad (2.11)$$

2.3 Results and Discussion

2.3.1 Wind Speed, Stability, and Roughness

To interpret analyses of the surface boundary layer, one must first be familiar with "typical" conditions at a commercial feedlot in western Kansas. Orthogonal distributions of wind speed (Figure 2.2) clearly show that typical conditions are characterized by very high-speed southerly winds. In the dominant southerly wind direction, average 30-min wind speeds were greater than 6 m s^{-1} more than 35% of the time, with an average daytime wind speed of 5 m s^{-1}, not uncommon for the cattle feeding region of the High Plains. The U.S. National Climatic Data Center ranks Dodge City, KS and Amarillo, TX, cities in the heart of the prime feedlot region, as the fifth and sixth windiest cities,

respectively, in the continental United States (National Climatic Data Center, 2006). Partially due to these high wind speeds, atmospheric stability (Figure 2.2) was near neutral 48% of the time with very few stable periods (around 25%). The other factor that helps sustain neutral stability, even under the often hot and dry feedlot conditions, is the significant amount of water deposited on the surface in the form of urine and fecal matter (Section 2.3.3 Carbon Dioxide, Latent Heat, and Sensible Heat Fluxes).

The displacement height for the feedlot, as computed using the Raupauch model (Eq. 2.8), was 0.65 m (0.54 x cattle height). Calculations of z_0 typically ranged between 2 and 6 cm with a mean of 4.1 ± 2.2 cm and a median of 3.6 cm. Considering that the feedlot surface is fairly smooth—it is basically a bare soil surface interspersed with cattle and feed bunks acting as bluff-rough elements—it is not surprising that the z_0 is small, similar to bluff-rough desert shrublands or sparsely vegetated vineyards (Stewart et al., 1994; Verhoef et al., 1997a). The georeferenced map of the feedlot showed that pens accounted for 72% of the area while roads and alleys, which are also smooth, accounted for 21% of the area. Flesch et al. (2007) reported z_0 values between 4 and 11 cm at a feedlot, similar to but slightly larger than results of this study.

2.3.2 Spectra, Cospectra, and Integration Inverval

Power spectra and cospectra were similar and showed the expected -2/3 and -4/3 slopes, respectively, in the inertial subrange (Figure 2.3). The cospectra slope was slightly less negative than -4/3, a feature commonly observed in other studies (Blanken et al., 1998). The spectra peak was near 0.01 for both scalars. There were no obvious differences between the CO_2 and T curves indicating isotropic turbulence, in other words, there was no systematic phase shift between CO_2 and T and no cospectral distortion (Velasco et al., 2005). For T and H, there was a slight upturn of both S_x and C_x at very high frequencies, a feature that could be the result of aliasing. Average wind speed was more than 6 m s^{-1} and H was more than 249 W m^{-2}, so temperature fluctuations of smaller, high-frequency eddies might not have been sampled adequately. However, this feature in the spectra would have no significant effect on flux measurement. The cospectra also were plotted on a semi-log scale so the area under sections of the curve was proportional to the covariance (i.e., flux) contributed by the corresponding

frequencies for each section (Figure 2.4). Again, good agreement between the C_x curves indicates that the same size eddies and turbulent processes were transferring both CO_2 and H. Evaluation of the C_x for ninety 30-min data periods at the feedlot during the summer of 2006 showed that 95% of the fluxes of both heat and mass were attributed to frequencies less than 5. Peak energy containing eddies were in the 0.2 to 0.3 band and the 0.04 to 0.06 band. Analysis of additional days showed that some had two peaks (Figure 2.4) while others did not. Calculation of wavelength ($\lambda = u/f$) indicates there might be discontinuity on the order of 50 to 70 m under certain conditions, a feature likely caused by the presence of the north-south road or alley in the footprint during southeast and southwest winds (Figure 2.1). In general, the power spectra and cospectra analyses suggest that emissions of trace gases from both the pen surface and cattle can be measured with EC and related methods (e.g., relaxed eddy accumulation). This analysis does not consider the effect of advection, a process that could be especially significant when estimating trace gas fluxes originating directly from the cattle (i.e., greater spatial variation).

Integration of the different sections of the cospectra curve was used to determine how much of the total flux could be attributed to frequencies greater than 1 Hz. Figure 2.5 shows the fraction of total flux accounted for by including progressively higher frequencies in the flux estimate; integration under the full 20 Hz cospectra was considered total flux. About two thirds of the total flux resulted from turbulent fluctuations less than 1 Hz. Of the remaining third, only 1.7% of H and 1.0% of F_c resulted from frequencies greater than 10 Hz. These data, collected 6 m above the surface, show that sampling at 10 Hz is acceptable when conducting EC measurements at feedlots. The same calculations performed with data collected 3 m above a grassland showed that 3 to 5% of the flux was attributed to frequencies greater than 10 Hz during high wind speeds. Thus, if sonic anemometers like the CSAT3 (i.e., 10 cm sample volume) are deployed at 3 m or less above a feedlot, sampling rates of 20 Hz or greater are advised to keep the uncertainty around the flux estimate low. Bosveld and Beljaars (2001) showed that lower sampling frequencies do not impact the expected value of eddy flux measurements but do increase uncertainty (i.e., noise) surrounding the estimate. Ogive plots showed almost no effect of low frequency eddies (Figure 2.6). In most cases,

integration intervals as low as 20 min were adequate to compute flux. However, the traditional 30-min integration interval for EC flux calculations appears acceptable. This is not surprising considering the relatively low height of the measurement (6 m) and prevalent high wind speeds at the shear-dominated site.

2.3.3 Carbon Dioxide, Latent Heat, and Sensible Heat Fluxes

Figure 2.7 shows diurnal composite curves of F_c for different periods during 2006. Emissions of CO_2 were extremely high with a fairly sharp, steady increase in F_c from around 3 mg m^{-2} s^{-1} at dawn to around 5 - 6 mg m^{-2} s^{-1} by late morning, roughly 10 to 15 times the maximum respiration rate observed with EC towers from agricultural crops or native ecosystems (e.g., Owensby et al., 2006). Fluxes remained fairly steady throughout the afternoon until early evening, when they began to slowly taper off to the predawn minimum, with the exception of a peak in flux just after dusk, likely due to increased cattle activity. Emissions from feedlot cattle vary, but assuming around 3000 L of CO_2 per day (Archibeque et al., 2007; Boadi et al., 2002), this would be an equivalent flux of about 4 mg m^{-2} s^{-1}, assuming a stocking density of 17 m^2 hd^{-1}, which agrees with measured F_c. It is important to note that the EC measured F_c includes both cattle and soil respiration. But, even under the most optimal conditions, soil respiration is typically less than 0.5 mg m^{-2} s^{-1}, so F_c from the feedlot was clearly dominated by cattle respiration. Kissinger et al. (2007) found that the average dry matter consumption of feedlot cattle was 10.3 kg $animal^{-1}$ d^{-1}, and of that total, 5.3 kg $animal^{-1}$ d^{-1} was harvested as manure. This leaves 5 kg $animal^{-1}$ d^{-1} of dry matter that must be accounted for in animal growth or respiration. Assuming the feed is 44% carbon and 20% of the animal growth is carbon (DeSutter and Ham, 2005), sample calculations showed expected F_c of about 4.4 mg m^{-2} s^{-1} on a pen surface basis. The footprint of the flux measurements was not all pen surface, so the expected EC measured flux could be slightly less than this value in most cases. Again, the average F_c in Figure 2.7 was 4 - 5 mg m^{-2} s^{-1}, which agreed closely with calculated values based on feeding data.

Figure 2.8 shows the composite curves for λE for the same periods. Latent heat fluxes exhibited the typical diurnal pattern with peaks ranging from 80 to 320 W m^{-2}, depending on the time of year. This area receives fairly low amounts of annual rainfall,

typically in short duration, high intensity events. The soil surface is visibly dry much of the time, except for the urine patches, so H_2O flux often is a reasonable estimate of cattle water consumption during dry periods. The exception would be immediately after precipitation or during the summer months when tanker trucks applied water to the feedlot to reduce dust emissions. The average daily λE for the fall period from September 1 - October 14 2007 was 7.9 MJ m^{-2}, equivalent to about 3.2 L m^{-2} of water. Assuming a stocking density of 17 m^2 $animal^{-1}$, this is about 55 L of water per head. Winchester and Morris (1956) showed the range of water consumption for feedlot cattle was typically between 20 and 80 L $animal^{-1}$ day^{-1}, and was dependent upon both animal weight and air temperature. Fluxes of H_2O were equivalent to 22.3 L $animal^{-1}$ day^{-1} during the winter period and 84.7 L $animal^{-1}$ day^{-1} during the summer period, consistent with ranges reported by Winchester and Morris (1956). Assuming the average annual rate of water consumption is 40 L $animal^{-1}$ d^{-1}, the amount of water deposited on the pen surface as urine and in fecal material would be, on average, 2.4 mm d^{-1} or 876 mm annually. Thus, the equivalent depth of water in the animal waste is about 1 1/2 times that received as precipitation.

Composite curves for H show there is very little difference in H between fall and summer periods (Figure 2.8), a sharp contrast with the differences seen in λE. During the summer, H is moderated by high λE, predominantly due to the large increase in cattle water consumption. The average daytime (1000-1600 LST) Bowen ratio for the summer period was 0.7 versus 1.1 for the fall and winter periods. One would suspect that the quasi-constant input of moisture moderates daily and seasonal variations in the stability of the surface boundary layer and the Bowen ratio.

2.3.4 Determining Fetch Requirements

Because F_c from the feedlot (3 to 6 mg m^{-2} s^{-1}) contrasted sharply with that from surrounding fields (-1.0 to 0.6 mg m^{-2} s^{-1}), the study provided an excellent opportunity for determining fetch requirements. When winds rotated too far to the east or west, the difference in magnitude between measured F_c and expected F_c (as defined by the composite) showed when the EC tower was sampling outside the feedlot (Figure 2.9). This indicator was used to fine-tune use of the Hsieh et al. (2000) model for footprint

testing. We were able to determine the percentage of the Hsieh-modeled source area that represented the actual fetch requirements for the feedlot. For each 30-min period, fetch requirements were calculated using a form of the Hsieh footprint model (Eq. 2.4) that predicted the distance from the tower representing a fraction of the source area of the flux measurement (i.e., distance from the tower representing 10, 20, . . . 90% of the source area, or $X_{10\%, 20\%, \ldots 90\%}$). If this distance extended beyond the feedlot boundary, that period was excluded from analysis. Intuitively, it would seem that $X_{100\%}$ would best represent fetch requirements. However, as the distance from the tower increases, the contribution of the source area decreases to a point where sensor resolution will mask any effects the additional contribution will have on the flux measurement. So, for all practical purposes, the actual fetch requirements will be some distance less than $X_{100\%}$. Hammerle et al. (2007) used $X_{90\%}$ to represent fetch requirements, but in fetch-limited situations like the feedlot, it is especially important that this distance be optimized to be as short as possible to retain more data while still effectively identifying bad periods.

Figure 2.10 shows measured F_c plotted against wind direction with different colors representing data retained after various footprint filtering criteria. Even though there is considerable scatter in places, the $X_{50\%}$ and $X_{60\%}$ filters clearly did not adequately filter out poor data because in the 240 to 270 degree direction, points are being retained that are showing the effects of dilution from outside the footprint (i.e., $F_c < 2$ mg m^{-2} s^{-1}). Conversely, the $X_{90\%}$ filter appeared to be too conservative, excluding a large number of points that are within range. It seems that an $X_{70\%}$ to $X_{80\%}$ footprint filtering criteria best filters the data and in the case of the feedlot (as would be the case in most fetch-limited situations), $X_{70\%}$ was chosen because it retained 25% more data than $X_{80\%}$ yet still appeared to adequately filter bad data. Under neutral conditions, $X_{70\%}$ was about 360m, representing a fetch to measurement height ratio of about 65:1. This is significantly less than the 100:1 conventional rule of thumb, but consistent with other field observations reporting minimum fetch to height ratios ranging from 15:1 to 75:1 (Baldocchi and Rao, 1995; Gash, 1986; Heilman et al., 1989; Irvine et al., 1997). Having a technique to determine the outer limit of the footprint is critical at a feedlot where almost every site will be fetch limited in certain wind directions.

2.3.5 Source Area Mapping

Fluxes measured with EC or other micrometeorological techniques will often need to be scaled to represent fluxes per unit animal or per unit pen area. Regulatory agencies want emissions factors expressed in these units so results can be scaled to regional levels using readily available data on cattle numbers. Also, fluxes per unit pen area are needed to compare the amount of nutrients delivered to the pens in the feed with the amount lost to the atmosphere. For example, if one could determine that 50% of the feed N was lost to the atmosphere as NH_3, it would be a useful scaling factor in determining bulk NH_3 contribution from feedlots over a large region. Finally, fluxes per unit area are needed by livestock producers and animal scientists so data can ultimately be expressed per animal, which is the experimental unit of interest when considering effects of diet and other aspects of CAFO management. Unfortunately, the footprint of a tower-based flux measurement contains surfaces other than pens (Figure 2.1). The GPS map of the feedlot showed that 72% of the surface represents pen areas where the animals are confined; the rest was composed of alleys used to move the cattle, roads for trucks delivering feed, and feed bunks (Table 2.1). These areas likely have negligible or very low emissions of CO_2, NH_3, and other compounds related to the cattle. Lagoons, buildings, and various other structures also represented a large fraction when the entire property was considered. Further complicating this issue is the dynamic nature of the feedlot operation; pens of cattle may vary by breed, weight, or sex; may be stocked at different densities; and can be fed different diets. In these situations, a thorough understanding of the source area footprint is needed to determine which pens are contributing to the flux signal or how the fluxes are being diluted by alleys and roads in the source area. Using an approximate analytical model developed by Hsieh et al. (2000), a two-dimensional cumulative flux footprint was developed (Figure 2.11) and clearly shows that EC flux measurement is dominated by a relatively small fraction of the feedlot. The three pens immediately south of the tower were responsible for 61% of the flux over a 6-month period, but represented less than 3% of the total feedlot area (Table 2.1). Thus, it would be especially important to know the characteristics of these pens. The model showed that, on average, alleys and roads contributed 10% and 2% of the flux signal, respectively.

Figure 2.12 shows the fraction of the EC measurements originating from pen surfaces (as modeled with $X_{70\%}$ representing the total flux) versus wind direction. When it was assumed that all fluxes of CO_2 originated from pens only and the raw EC fluxes were scaled up to pen area fluxes, results showed that, on average, fluxes were increased by 11%, bringing average F_c up to 4.4 - 5.6 mg m^{-2} s^{-1}. When winds were more easterly, more of the footprint was occupied by alleys (less pen area in the footprint) and fluxes were scaled up by as much as 31% during certain 30-min periods. This approach for scaling flux measurement to account for non-pen surfaces in the footprint depends on the suitability of the Hsieh model and on the assumption of zero-flux in the non-pen areas. While simplistic, it represents an important first step in trying to scale results in a manner consistent with the nutrient balance of the pen and individual animals. This is crucial in a feedlot setting where EC measurements will likely be compared with feeding data.

2.4 Conclusions

Micrometeorological techniques are very useful tools for making emissions measurements, but the underlying theory behind these techniques necessitates a large, steady-state, homogeneous surface. The goal of this research was to assess the feasibility of using EC and other micrometeorological techniques for measuring emissions from a less than ideal surface - a cattle feedlot. To accomplish this, we characterized the surface boundary layer of a commercial feedlot in western Kansas. Typically, this feedlot experienced high wind speeds and near-neutral atmospheric stability, so extrapolating from measurements made under calm and/or stable conditions is not advised as they would be very unrepresentative of typical conditions at feedlots in this region. Data showed a roughness length of 3.6 cm and a modeled displacement height of 65 cm. Thus, the surface is aerodynamically smooth as sensed from above, but one cannot ignore the contribution of the cattle (i.e., moving bluff bodies). Power spectra and cospectra showed the expected -2/3 and -4/3 slopes, respectively, in the inertial subrange, and there was no sign of turbulent features that would prohibit the use of EC or related techniques. In terms of daily emission rates per head, EC measurements of F_c and λE agreed with other studies measuring cattle respiration or water consumption. The percentage of the Hsieh modeled source area that represented actual fetch requirements for the feedlot was

about 70% to 80%. Under neutral conditions, $X_{70\%}$ was about 360 m, representing a fetch to measurement height ratio of about 65:1. Even with a 6-m measuring height, the source area of the EC flux measurements was dominated by a small portion of the feedlot, with 61% of the signal originating from the three pens immediately south of the tower. Therefore, it would be especially important to know the characteristics of those pens when relating flux measurements back to nutrient loading, cattle diets, or stocking density. Finally, for researchers interested in flux measurements in terms of pen surface, the effects of non-pen surfaces on the measurements could be significant. Raw EC fluxes were typically increased by 11% to represent pen area fluxes but were sometimes scaled up by as much as 31%. Indications are that micrometeorological techniques can be successfully applied to cattle feedlots in the High Plains. Results of this research provide guidance for applying these techniques to cattle feedlots and offer insight into challenges that must be faced in many fetch-limited, heterogeneous situations.

References

Adams, J.R., Farran, T.B., Erickson, G.E., Klopfenstein, T.J., Macken, C.N., Wilson, C.B., 2004. Effect of organic matter addition to the pen surface and pen cleaning frequency on nitrogen mass balance in open feedlots. J. Anim. Sci. 82, 2153-2167.

American Society of Agricultural and Biological Engineers, 2006. Dimensions of livestock and poultry. ASAE Livestock Dimension and Configuration Factors Subcommittee, ASAE Structures and Environ. Division Tech. Committee. ASAE Standard D321.2 MAR1985 (R2006). ASABE, St. Joseph, MI.

Archibeque, S.L., Freetly, H.C., Cole, N.A., Ferrell, C.L., 2007. The influence of oscillating dietary protein concentrations on finishing cattle. II. nutrient retention and ammonia emissions. J. Anim. Sci. 85, 1496-1503.

Baek, B.-H., Todd, R., Cole, N.A., Koziel, J.A., 2006. Ammonia and hydrogen sulphide flux and dry deposition velocity estimates using vertical gradient method at a commercial beef cattle feedlot. Int. J. Global Env. Issues 6(2/3), 189-203.

Baldocchi, D.D. and Rao, K.S., 1995. Intra-field variability of scalar flux densities across a transition between a desert and an irrigated potato field. Boundary-Layer Meteorol. 76(1-2), 109-136.

Beauchemin, K.A., McGinn, S.M., 2005. Methane emissions from feedlot cattle fed barley or corn diets. J. Anim. Sci. 83, 653-661.

Beauchemin, K.A., McGinn, S.M., 2006. Methane emissions from beef cattle: effects of fumaric acid, essential oil, and canola oil. J. Anim. Sci. 84, 1489-1496.

Bierman, S., Erickson, G.E., Klopfenstein, T.J., Stock, R.A., Shain, D.H., 1999. Evaluation of nitrogen and organic matter balance in the feedlot as affected by level and source of dietary fiber. J. Anim. Sci. 77, 1645-1653.

Blanken, P.D., Black, T.A., Neumann, H.H., Den Hartog, G., Yang, P.C., Nesic, Z., Staebler, R., Chen, W., Novak, M.D., 1998. Turbulent flux measurements above and below the overstory of a boreal aspen forest. Boundary-Layer Meteorol. 89, 109-140.

Boadi, D.A., Wittenberg, K.M., Kennedy, A.D., 2002. Validation of the sulphur hexafluoride (SF_6) tracer gas technique for measurement of methane and carbon dioxide production by cattle. Can. J. Anim. Sci. 82, 125-131.

Boadi, D.A., Wittenberg, K.M., Scott, S.L., Burton, D., Buckley, K., Small, J.A., Ominski, K.H., 2004. Effect of low and high forage diet on enteric and manure pack greenhouse gas emissions from a feedlot. Can. J. Anim. Sci. 84, 445-453.

Bosveld, F.C., Beljaars, A.C.M., 2001. The impact of sampling rate on eddy-covariance flux estimates. Ag. For. Meteorol. 109(1), 39-45.

Businger, J.A., Wyngaard, J.C., Izumi, Y., Bradley, E.F., 1971. Flux-profile relationships in the atmospheric surface layer. J. Atmos. Sci. 28, 181-189.

Casey, K.D., Bicudo, J.R., Schmidt, D.R., Singh, A., Gay, S.W., Gates, R.S., Jacobson, L.D., Hoff, S.J., 2006. Air quality and emissions from livestock and poultry production/waste management systems. *In* Rice, J.M., Caldwell, D.F., Humenik, F.J. (ed.) Animal Agriculture and the Environment: National Center for Manure and Animal Waste Management White Papers. ASABE: Pub. Number 913C0306. St. Joseph, MI .

Cole, N.A., Todd, R.W., Parker, D.B., Rhoades, D.B., 2007. Challenges in using flux chambers to measure ammonia emissions from simulated open feedlot pen surfaces and retention ponds. *In* Proceedings of the ASABE International Symposium on Air Quality and Waste Management for Agriculture, September 16-19, 2007, Broomfield, Colorado. CD-ROM.

DeSutter, T.M., Ham, J.M., 2005. Lagoon-biogas emissions and carbon balance estimates of a swine production facility. J. Environ. Qual. 34, 198-206.

Dyer, A.J., 1974. A review of flux-profile relationships. Boundary-Layer Meteorol. 7, 363-372.

Ellis, S., Webb, J., Misselbrook, T., Chadwick, D., 2001. Emission of ammonia (NH_3), nitrous oxide (N_2O) and methane (CH_4) from a dairy hardstanding in the UK. Nut. Cyc. Agroecosys. 60, 115-122.

Erickson, G.E., Klopfenstein, T.J., 2001a. Managing N inputs and the effect on N losses following excretion in open-dirt feedlots in Nebraska. *In* Optimizing Nitrogen Management in Food and Energy Production and Environmental Protection:

Proceedings of the 2nd International Nitrogen Conference on Science and Policy. TheScientificWorld 1(S2), 830-835.

Erickson, G.E., Klopfenstein, T.J., 2001b. Nutritional methods to decrease N losses from open-dirt feedlots in Nebraska. *In* Optimizing Nitrogen Management in Food and Energy Production and Environmental Protection: Proceedings of the 2nd International Nitrogen Conference on Science and Policy. TheScientificWorld 1(S2), 836-843.

Farran, T.B., Erickson, G.E., Klopfenstein, T.J., Macken, C.N., Lindquist, R.U., 2006. Wet corn gluten feed and alfalfa hay levels in dry-rolled corn finishing diets: effects on finishing performance and feedlot nitrogen mass balance. J. Anim. Sci. 84, 1205-1214.

Flesch, T.K., Wilson, J.D., Harper, L.A., Todd, R.W., Cole, N.A., 2007. Determining ammonia emissions from a cattle feedlot with an inverse dispersion technique. Agric. For. Meteorol. 144, 139-155.

Foken, T., Wichura, B., 1996. Tools for quality assessment of surface-based flux measurements. Ag. For. Meteorol. 78, 83-105.

Foken, T., Göckede, M., Mauder, M., Mahrt, L., Amiro, B., Munger, W., 2004. Post-field data quality control. *In* Lee et al. (ed.) Handbook of micrometeorology: a guide for surface flux measurement and analysis. Kluwer Academic Publishers, The Netherlands.

Gash, J.H.C. 1986. Observations of turbulence downwind of a forest-heath transition. Boundary-Layer Meteorol. 36, 227-237.

Hammerle, A., Haslwanter, A., Schmitt, M., Bahn, M., Tappeiner, U., Cernusca, A., Wohlfahrt, G., 2007. Eddy covariance measurements of carbon dioxide, latent and sensible energy fluxes above a meadow on a mountain slope. Boundary-Layer Meteorol. 122, 397-416.

Harper, L.A., Denmead, O.T., Freney, J.R., Byers, F.M., 1999. Direct measurements of methane emissions from grazing and feedlot cattle. J. Anim. Sci. 77, 1392-1401.

Heilman, J.L., Brittin, C.L., Neale, C.M.U., 1989. Fetch requirements for Bowen ratio measurements of latent and sensible heat fluxes. Agric. For. Meteorol. 44, 261–273.

Hsieh, C., Katul, G., Chi, T., 2000. An approximate analytical model for footprint estimation of scalar fluxes in thermally stratified atmospheric flows. Adv. Water Res. 23, 765-772.

Hutchinson, G.L., Mosier, A.R., Andre, C.E., 1982. Ammonia and amine emissions from a large cattle feedlot. J. Env. Qual. 11(2), 288-293.

Irvine, M.R., Gardiner, B.A., Hill, M.K., 1997. The evolution of turbulence across a forest edge. Boundary-Layer Meteorol. 84, 467-496.

Kaharabata, S.K., Schuepp, P.H., Desjardins, R.L., 2000. Estimating methane emissions from dairy cattle housed in a barn and feedlot using an atmospheric tracer. Env. Sci. Tech. 34, 3296-3302.

Kaimal, J.C., Finnigan, J.J., 1994. Atmospheric Boundary Layer Flows: There Structure and Measurement. Oxford University Press, Inc., New York, NY.

Kissinger, W.F., Koelsch, R.K., Erickson, G.E., Klopfenstein, T.J., 2007. Characteristics of manure harvested from beef cattle feedlots. Appl. Eng. Agric. 23(3), 357-365.

Lamb, B.K., McManus, J.B., Shorter, J.H., Kolb, C.E., Mosher, B., Harriss, R.C., Allwine, E., Blaha, D., Howard, T., Guenther, A., Lott, R.A., Siverson, R., Westberg, H., Zimmerman, P., 1995. Development of atmospheric tracer methods to measure methane emissions from natural gas facilities and urban areas. Env. Sci. Tech. 29, 1468-1479.

Lee, X., Massman, W., and Law, B. 2004. Handbook of Micrometeorology: A Guide for Surface Flux Measurement and Analysis. Dordrecht, The Netherlands: Kluwer Academic Publishers. 250 p.

McGinn, S.M., Beauchemin, K.A., Coates, T., Colombatto, D., 2004. Methane emissions from beef cattle: effects of monensin, sunflower oil, enzymes, yeast, and fumaric acid. J. Anim. Sci. 82, 3346-3356.

McGinn, S.M., Beauchemin, K.A., Iwaasa, A.D., McAllister, T.A., 2006a. Assessement of the sulfur hexafluoride (SF_6) tracer technique for measuring enteric methane emissions from cattle. J. Env. Qual. 35, 1686-1691.

McGinn, S.M., Flesch, T.K., Harper, L.A., Beauchemin, K.A., 2006b. An approach for measuring methane emissions from whole farms. J. Env. Qual. 35, 14-20.

McGinn, S.M., Flesch, T.K., Crenna, B.P., Beauchemin, K.A., Coates, T., 2007. Quantifying ammonia emissions from cattle feedlot using a dispersion model. J. Environ. Qual. 36, 1585-1590.

Misselbrook, T.H., Webb, J., Chadwick, D.R., Ellis, S., Pain, B.F., 2001. Gaseous emissions from outdoor concrete yards used by livestock. Atmos. Env. 35, 5331-5338.

Misselbrook, T.H., Webb, J., Gilhespy, S.L., 2006. Ammonia emissions from outdoor concrete yards used by livestock—quantification and mitigation. Atmos. Env. 40, 6752-6763.

Moncrieff, J., Clement, R., Finnigan, J., Meyers, T., 2004. Averaging, detrending, and filtering of eddy covariance time series. *In* Lee et al. (ed.) Handbook of micrometeorology: a guide for surface flux measurement and analysis. Kluwer Academic Publishers, The Netherlands.

National Agricultural Statistics Service, United States Department of Agriculture, 2004. Cattle: Final Estimates 1999-2003. United States Government Printing Office. Washington D.C. http://usda.mannlib.cornell.edu/usda/nass/SB989/sb989.pdf

National Climatic Data Center, NOAA Satellite an Information Service, 2006. Comparative Climatic Data Publication. Wind—Average Speed (MPH). http://www.ncdc.noaa.gov/oa/climate/online/ccd/wndspd.txt

National Research Council, 2003. Air Emissions From Animal Feeding Operations: Current Knowledge, Future Needs. The National Academies Press. Washington D.C.

Owensby, C.E., Ham, J.M., Auen, L.M., 2006. Fluxes of CO_2 from grazed and ungrazed tallgrass prairie. Rangeland Ecol. Manag. 59, 111-127.

Prueger, J.H., Kustas., W.P., 2005. Aerodynamic principles of flux-profile relationships. In *Micrometeorology in agricultural systems*, Madison, WI. Agronomy Monograph 47, ASA, CSSA, SSSA.

Raupach, M.R. 1994. Simplified expressions for vegetation roughness length and zero-plane displacement height as functions of canopy height and area index. Boundary-Layer Meteorol. 71, 211-216.

Shah, S.B., Westerman, P.W., Arogo, J., 2006. Measuring ammonia concentrations and emissions from agricultural land and liquid surfaces: a review. J. of Air and Waste Management Association. 56, 945-960.

Steinfeld, H., Gerber, P., Wassenaar, T., Castel, V., Rosales, M., de Haan, C., 2006. Livestock's Long Shadow: Environmental Issues and Options. Food and Agriculture Organization of the United Nations.

Stewart, J.B., Kustas, W.P., Humes, K.S., Nichols, W.D., Moran, M.S., De Bruin, H.A.R., 1994. Sensible heat flux-radiometric surface temperature relationship for eight semiarid areas. J. Appl. Meteorol. 33, 1110-1117.

Todd, R.W., Cole, N.A., Harper, L.A., Flesch, T.K., 2007. Flux-gradient estimates of ammonia emissions from beef cattle feedyard pens. *In* Proceedings of the ASABE International Symposium on Air Quality and Waste Management for Agriculture, September 16-19, 2007, Broomfield, Colorado. CD-ROM.

van Aardenne, J.A., Dentener, F.J., Olivier, J.G.J., Klein Goldewijk, C.G.M., Lelieveld, J., 2001. A 1 x 1 resolution data set of historical anthropogenic trace gas emissions for the period 1890-1990. Global Biogeochemical Cycles. 15(4), 909-928.

Velasco, E., Pressley, S., Allwine, E., Westberg., Lamb, B., 2005. Measurement of CO_2 fluxes from the Mexico City urban landscape. Atmos. Environ. 39(38), 7433-7446.

Verhoef, A., De Bruin, A.R., Van Den Hurk, B.J.J.M., 1997a. Some practical notes on the parameter kB^{-1} for sparse vegetation. J. Appl. Meteorol. 36, 560-572.

Verhoef, A., McNaughton, K.G., Jacobs, A.F.G., 1997b. A parameterization of momentum roughness length and displacement height for a wide range of canopy densities. Hydrology and Earth System Sciences. 1, 81-91.

Winchester, D.F., Morris, M.J., 1956. Water intake rates of cattle. J. Anim. Sci. 15, 722-740.

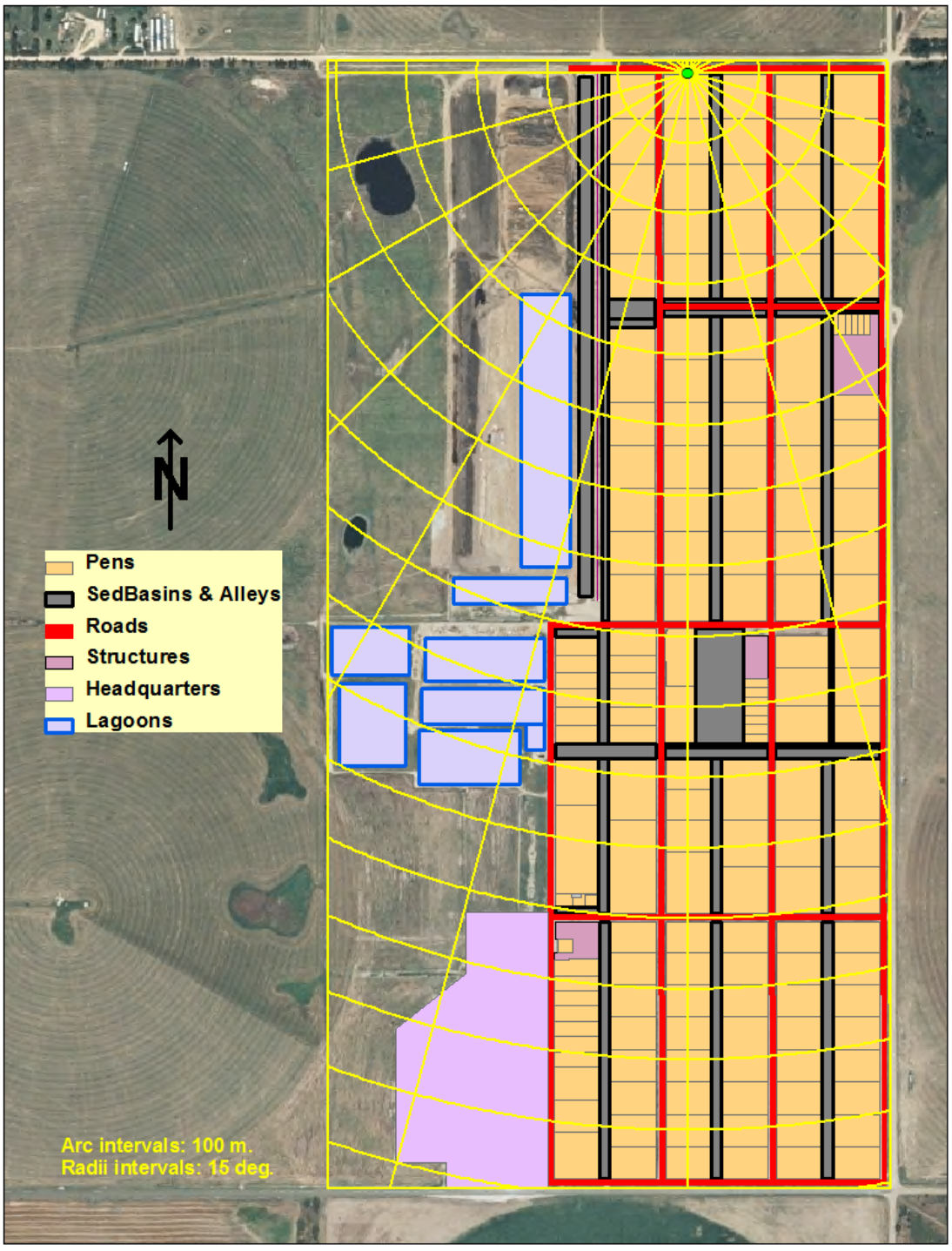

Figure 2.1 Map of the feedlot showing configuration of the pens and the location of the tower along the north edge of the feedlot.

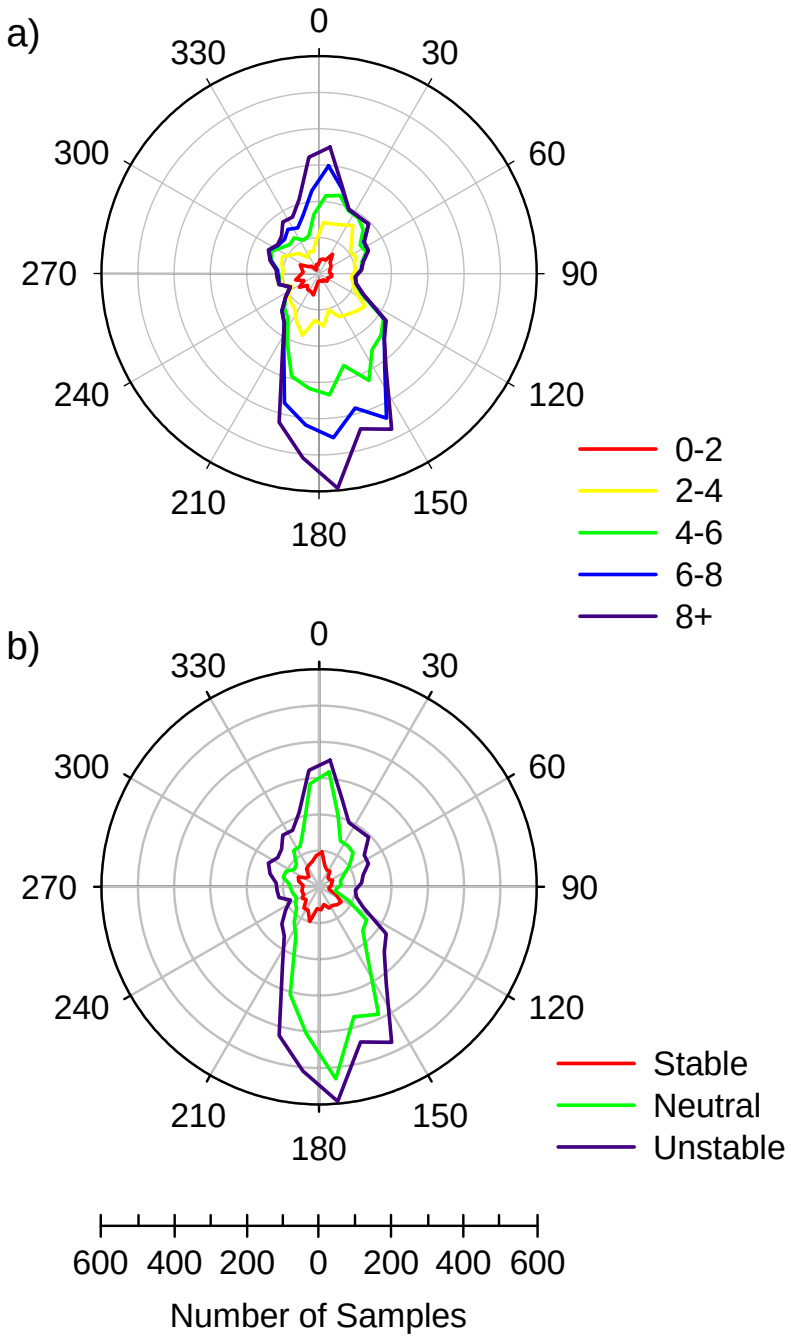

Figure 2.2 Polar plots for 30-min averages of a) wind speed (m s^{-1}) and b) atmospheric stability versus wind direction for days of year 194-365, 2006, where L>100 is stable, |L|>100 is neutral, and L<-100 is unstable. Stacked configuration similar to stacked bar charts.

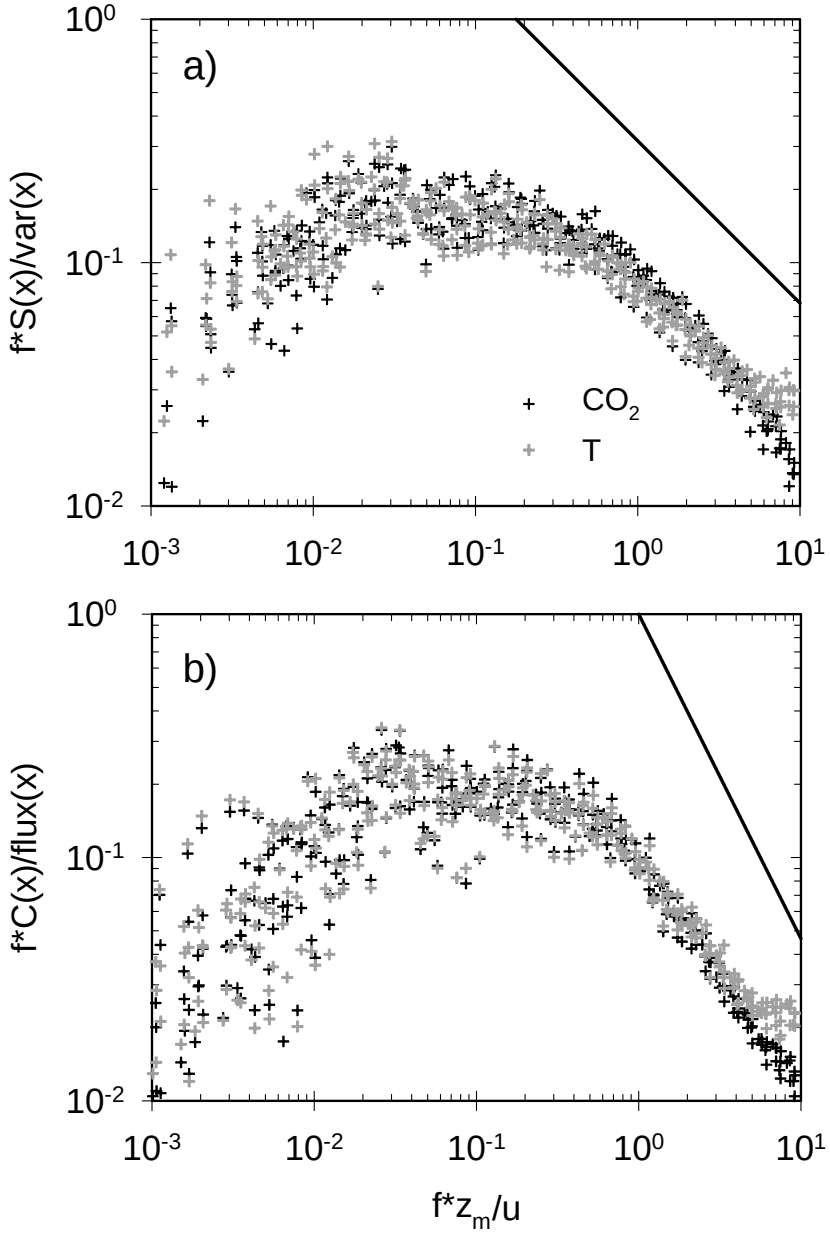

Figure 2.3 (a) Power density spectra for CO_2 and air temperature (T) and (b) cospectra of vertical wind speed with CO_2 and T. Data are shown for eight 30-min periods between 1000 and 1400 LST on August 30, 2006. On average, wind speed was 6.4 m s^{-1}, CO_2 flux was 5.4 mg m^{-2} s^{-1}, and sensible heat flux was 250 W m^{-2}. The -2/3 and -4/3 sloped reference lines are added to the power spectra and cospectra plots, respectively.

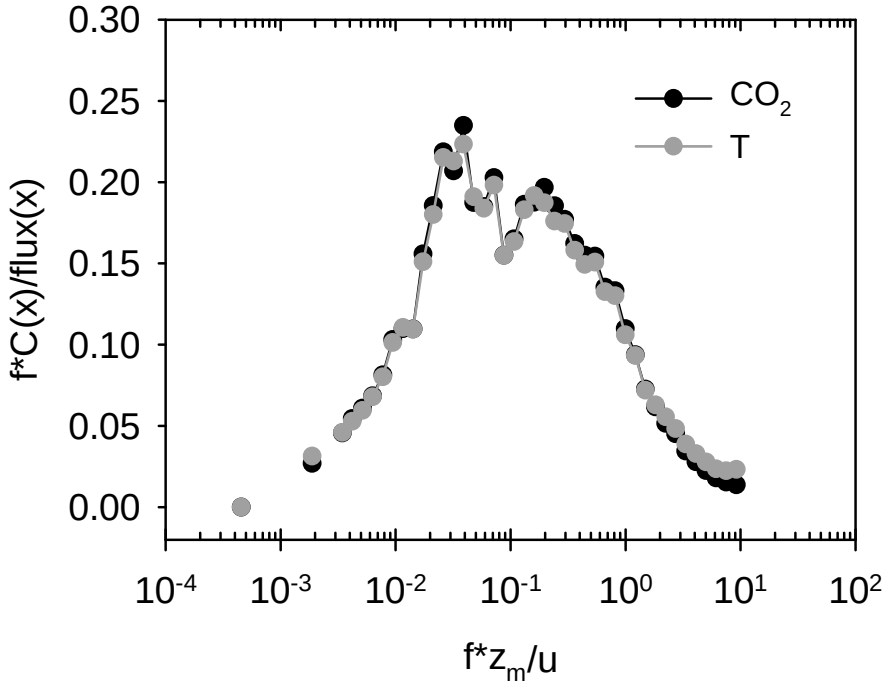

Figure 2.4 Semi-log plot of the CO_2 and T cospectra (same data as Fig. 2.3b). For clarity, data were bin-averaged for 50 equally spaced intervals on the log x-axis.

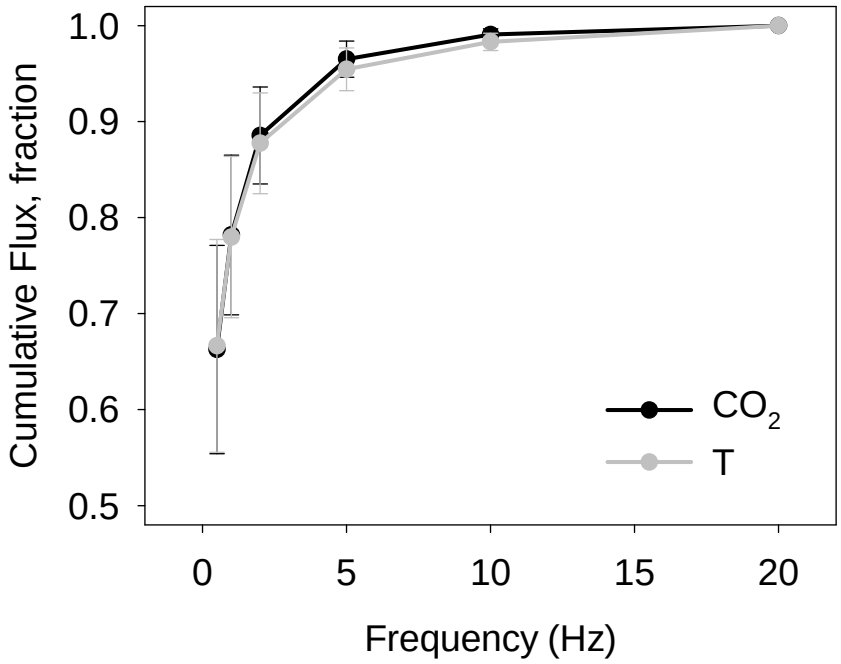

Figure 2.5 Cumulative fraction of total F_c and H attributed to frequencies greater than 1 Hz. Data show the fraction of total flux accounted for by including progressively higher frequencies. Integration under the full 20 Hz cospectra was considered total flux. Time series data were collected at 6 m, and results represent the composite of selected days in July, August, and September with a mean wind speed of 7.6 m s^{-1}. Error bars represent ± one standard error.

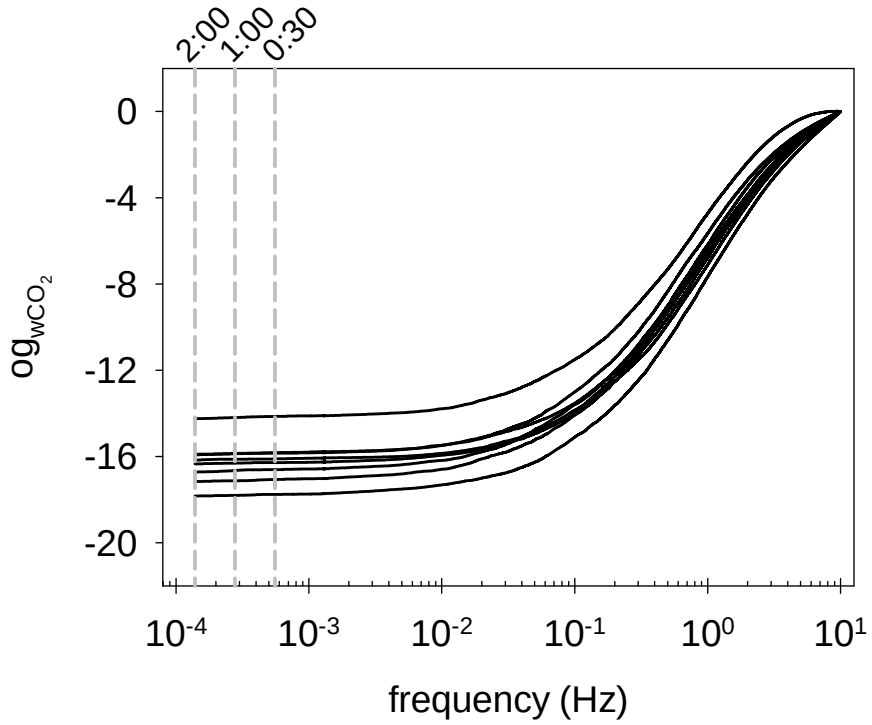

Figure 2.6 Ogives for H and F_c for the same days used in Figure 2.5. The vertical lines represent integration intervals of 30, 60, and 120 minutes. The point where the ogive line becomes asymptotic is an indication that turbulence with longer periods are not affecting flux.

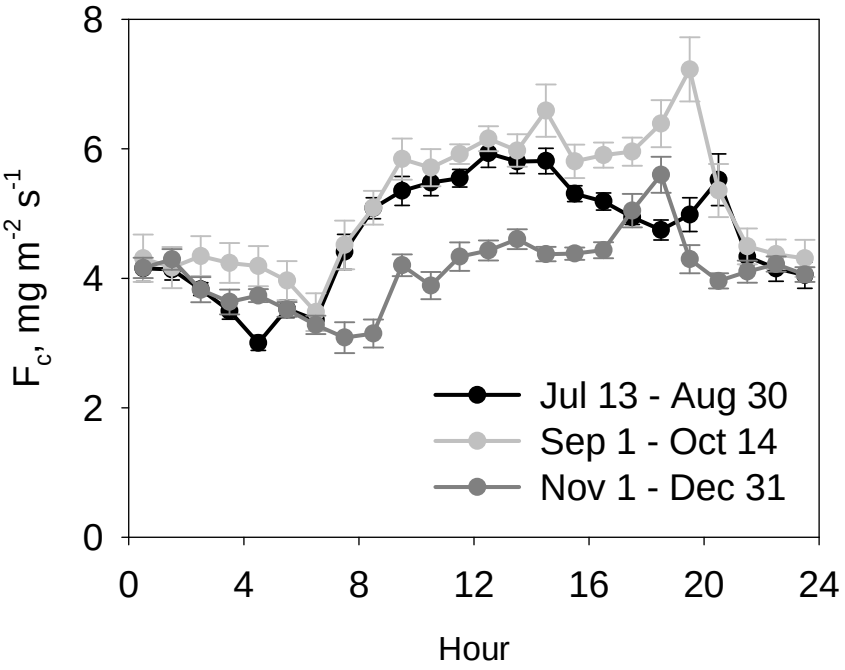

Figure 2.7 Composite diurnal curve for CO_2 flux averaged using only those 30-min periods where it could be reasonably assumed that fetch was adequate (atmospheric stability was either neutral or unstable and based on wind direction, there was a fetch:height ratio of at least 100:1). Error bars represent ± one standard error.

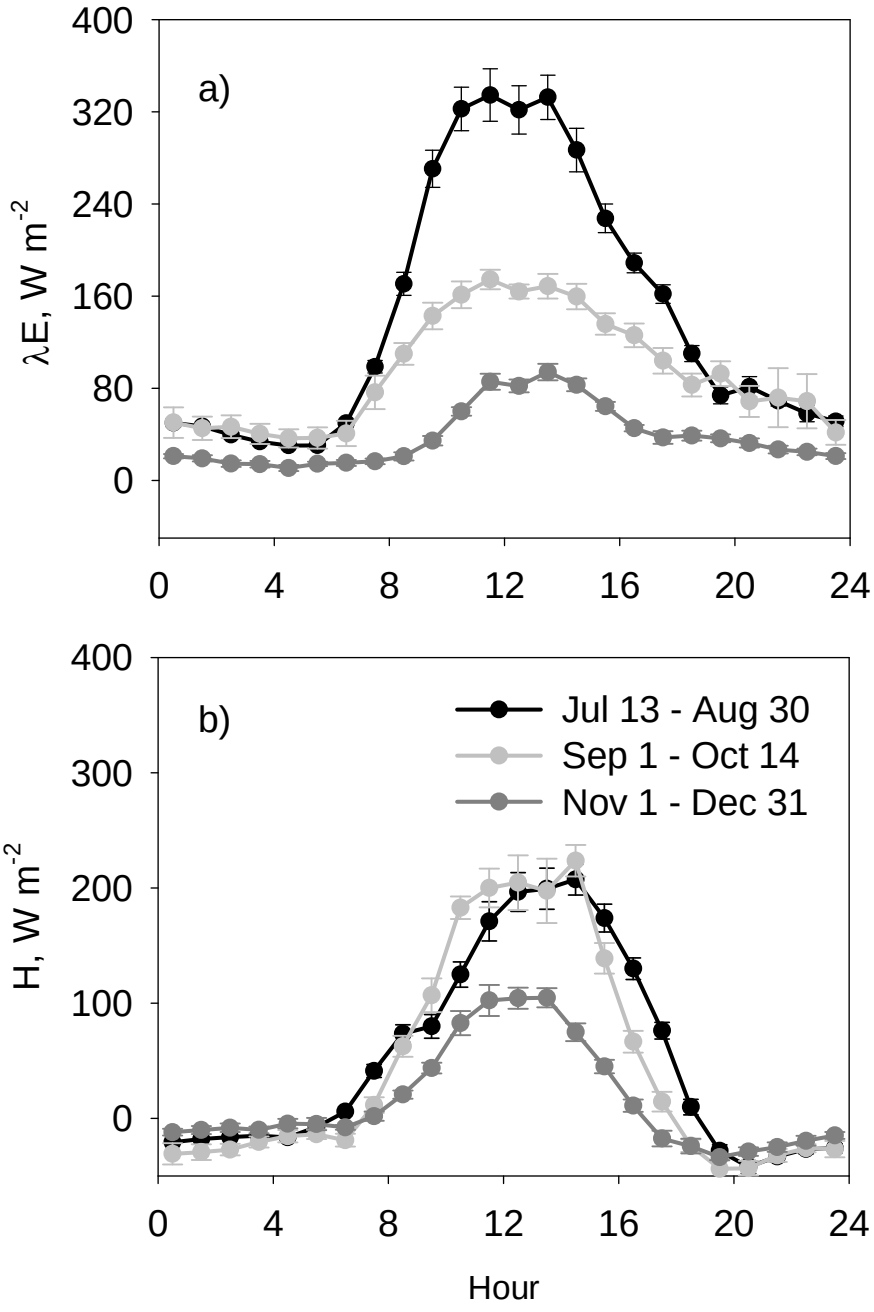

Figure 2.8 Composite diurnal curves for (a) latent and (b) sensible heat fluxes averaged using only those 30-min periods where it could be reasonably assumed that fetch was adequate (atmospheric stability was either neutral or unstable and based on wind direction, there was a fetch:height ratio of at least 100:1). Error bars represent ± one standard error.

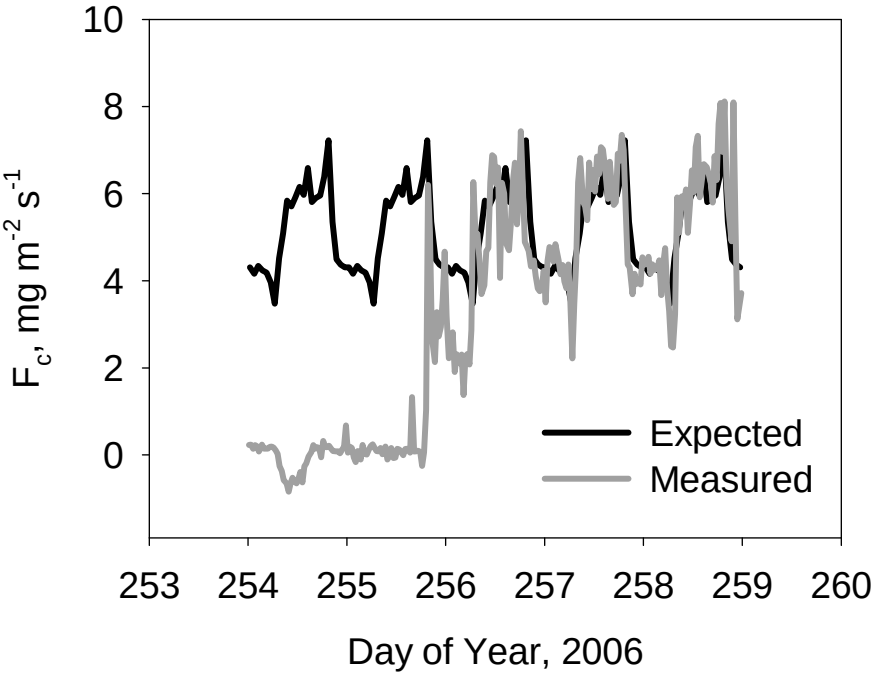

Figure 2.9 Time series of the expected F_c (composite F_c from Fig. 2.7) and the EC measured F_c. Deviations between the two clearly show when the EC tower is sampling outside the feedlot footprint.

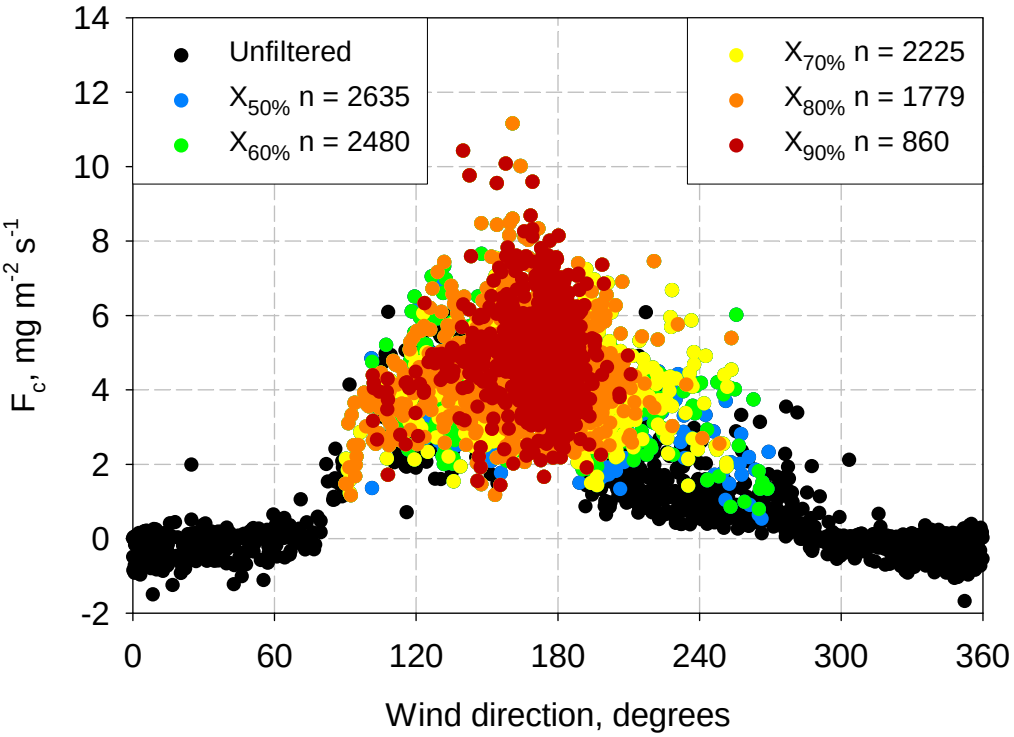

Figure 2.10 Eddy covariance measured F_c plotted against wind direction with different colors representing data that were retained (considered good) after various footprint filtering criteria were used. For example, $X_{70\%}$ represents 30-min periods retained (i.e., n = 2225) where 70% of the source area was within the boundary of the feedlot, according the model of Hsieh et al. (2000).

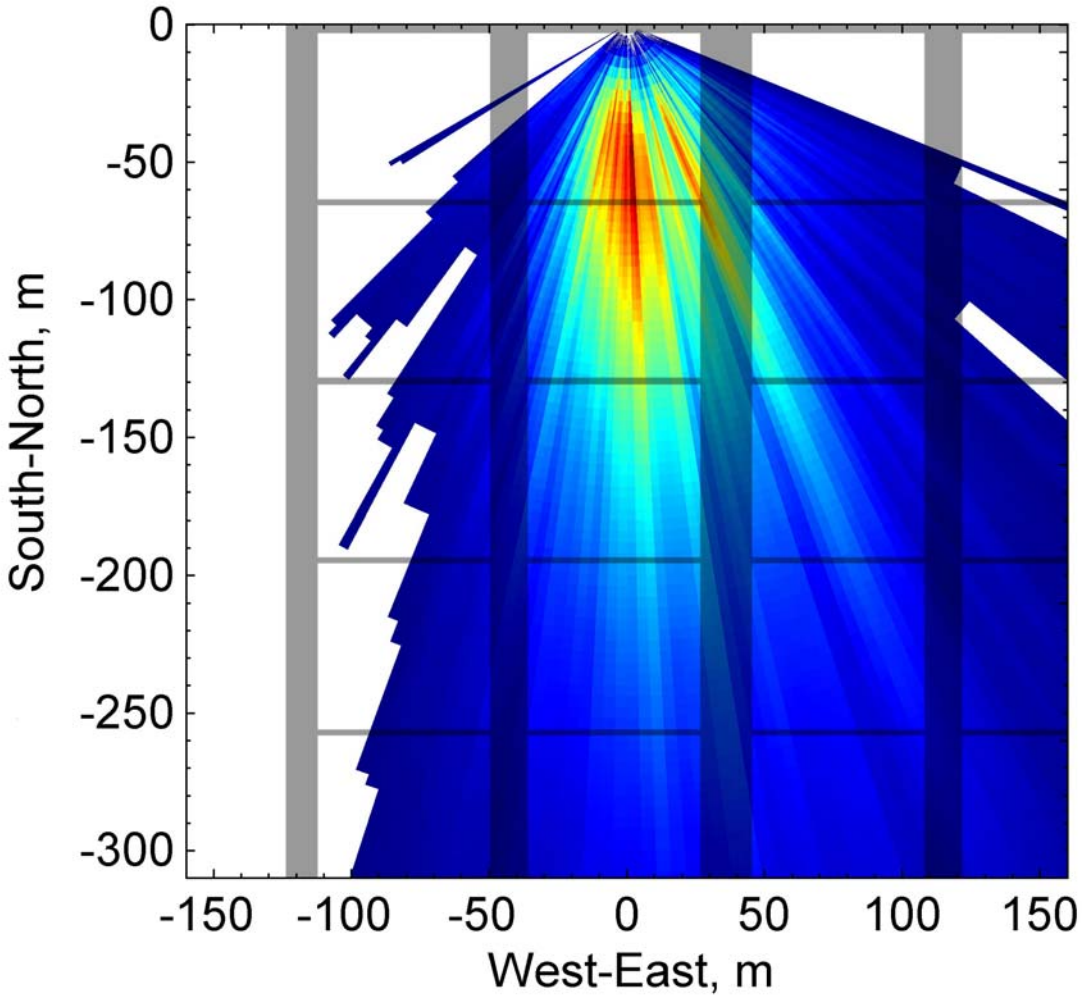

Figure 2.11 Map of the Hsieh modeled source area of EC measurements of flux for the period from July 13 to December 31, 2006. Gray lines show the pen boundaries (See Figure 2.1). Red indicates heavily sampled areas.

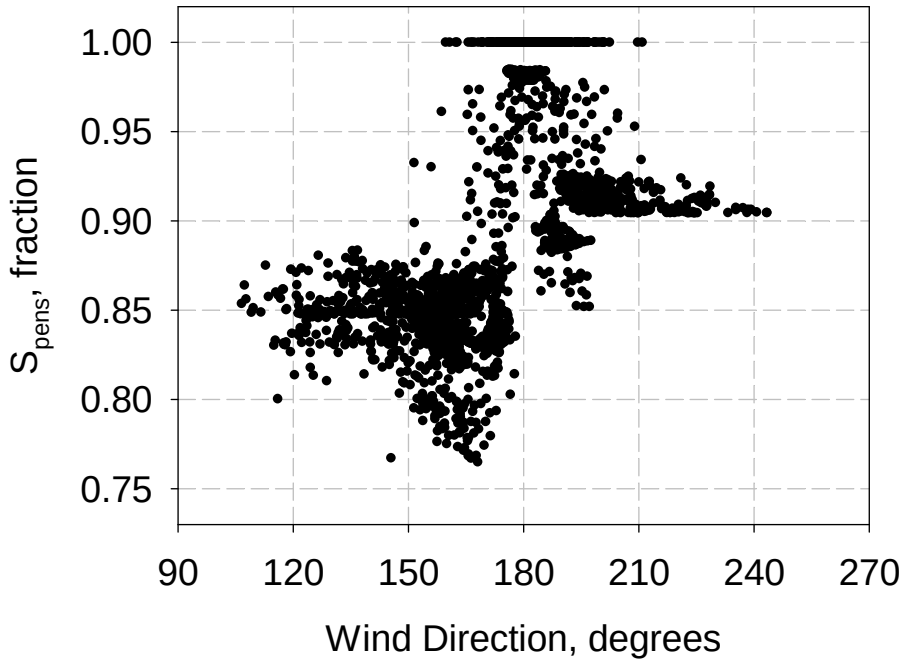

Figure 2.12 Fraction of the weighted EC source area attributed to pen surfaces, S_{pens} (as modeled with $X_{70\%}$ representing the total flux) versus wind direction for the period from July 13 to December 31, 2006.

Table 2.1 Surface area and relative contribution to EC flux measurements from pens, alleys, and roads.

Feedlot Feature	Surface Area, %	Contribution to Measured Flux, %
Pen A*	0.8	35.0
Pen B*	0.8	18.8
Pen C*	0.8	7.5
Remaining Pens	69.5	25.5
Pen Subtotal	71.9	86.8
Sediment Basins & Alleys	14.0	9.5
Roads	7.1	2.3
Other**	6.9	1.5
TOTAL	100.0	100.0

*Pens "A", "B", and "C" are the closest pens directly south of the tower (Figure 2.11).

**"Other" denotes structures, feed bunks, and otherwise unassigned areas.

CHAPTER 3 - Adaptation of a Speciation Sampling Cartridge for Measuring Ammonia Flux from Cattle Feedlots Using Relaxed Eddy Accumulation

3.1 Introduction

A report by the National Research Council ranked ammonia (NH_3) as the most important emission from confined animal feeding operations (CAFOs) at regional and national scales (National Research Council, 2003). Regulations regarding regional haze prompted the United States Environmental Protection Agency (USEPA) to include NH_3 in the consolidated emission inventory reporting requirements because NH_3 can convert to NH_4^+ aerosols, which contribute to $PM_{2.5}$ (particulate matter with an aerodynamic diameter less than 2.5μm), a major contributor to regional haze (USEPA, 2002). Additionally, researchers have shown that NH_3 deposition can lead to soil acidification (ApSimon et al., 1987; Brunet et al., 1998) and shifts in species composition (Bobbink et al., 1998; Pittcairn et al., 1998). The livestock industry contributes an estimated 64% of global anthropogenic NH_3 emissions (Steinfeld et al., 2006), and cattle feedlots are a large component of the livestock industry, with nearly 30 million animals marketed each year (National Agricultural Statistics Service, 2004), so obtaining accurate estimates of emissions from feedlots is important.

Micrometeorological methods (e.g., eddy covariance (EC), relaxed eddy accumulation (REA)) are often considered the best methods for measuring fluxes from CAFOs (Shah et al., 2006) and would be ideal in feedlot situations because they provide areally averaged flux measurements for large areas without disturbing the surface. Eddy covariance is the most desirable method because it provides a direct measure of flux; the flux density of a compound is expressed statistically as the covariance between deviations in the vertical wind speed and the mixing ratio of the compound of interest. This method is commonly used for measuring carbon dioxide and water vapor fluxes; however, high

frequency measurements are needed, dictating the need for a fast-response analyzer (i.e., 10 to 20 Hz), which disallows its use for certain compounds, including NH_3.

Relaxed eddy accumulation is an alternative to EC that avoids the need for a fast-response analyzer. Resolved by Businger and Oncely (1990), REA is a form of conditional sampling whereby samples of up- and down-moving eddies are sorted with high speed valves and can be analyzed with slower response analyzers or wet chemistry techniques. The mass flux, F (kg m^{-2} s^{-1}), is calculated as:

$$\overline{F} = \beta \rho \sigma_w \left(\overline{\chi^+} - \overline{\chi^-} \right) \tag{3.1}$$

where $\chi^{+/-}$ is the mixing ratio of the compound of interest for the up-moving and down-moving eddies, respectively (kg kg^{-1}); ρ is air density (kg m^{-3}); β is a dimensionless relaxation factor; σ_w is the standard deviation of the vertical wind speed (m s^{-1}); and overbars represent time-averages. Essentially, a sonic anemometer measures the three dimensional wind speed, including the vertical velocity, w. If an eddy with upward trajectory is detected (w>0), the upward valve is activated and air is diverted to the up-eddy reservoir. If an eddy with downward trajectory is detected (w<0), the downward valve is activated and air is diverted to the down-eddy reservoir. Often times the difference between the mixing ratios of the up- and down-moving eddies is very small so in practice, a deadband (db) is used; if the vertical wind speed is near zero (|w|<db), air is not sampled, increasing the difference between the up-moving and down-moving mixing ratios. An overview of REA is provided by McInnes and Heilman (2005).

Several studies have successfully used REA to measure fluxes of various trace gases and aerosols (Beverland et al., 1996; Bowling et al., 1998; Christensen et al., 2000; Gaman et al., 2004; Guenther et al., 1996; Valentini et al., 1997). However, it is difficult to design an REA sampling system for NH_3 because of its reactive nature (i.e., interaction with tubing walls). A few studies have measured atmospheric NH_3 and NH_4^+ concentrations using glass denuder tubes (Ferm, 1979; Sutton et al., 2001). These systems have promise because they can selectively trap gaseous NH_3 only (no NH_4^+) and the NH_3 does not have to travel through tubing—it is immediately trapped by the coating of the glass denuders. Zhu et al. (2000) used denuder tubes in an REA system for measuring NH_3 fluxes from a fertilized corn field, but in CAFO situations where NH_3

concentrations are so high (e.g., 300-600 μg m^{-3}), this is not feasible because the denuders would saturate within seconds.

A commercially available product that might be a solution to this problem is the Chemcomb Speciation Sampling Cartridge (model 3500, Thermo Scientific, Waltham, MA). The main components of this product are a well-characterized inlet and impactor plate with a 2.5μm or 10μm particle size cutoff, a series of glass honeycomb denuders, and a filterpack outlet. The honeycomb configuration of the denuders has the advantage of a very high capacity in a relatively small, compact package. Typically, each cartridge contains either 2 or 4 denuders, with 1 (or 2) denuders coated with a base for trapping acidic gases and 1 (or 2) denuders coated with an acid for trapping basic gases. Because the denuders selectively trap gaseous compounds, the filterpack at the outlet can house various filters that will retain particulates, allowing for the determination of gaseous and aerosol phases of compounds separately. The denuder-filterpack design offers flexibility in that virtually any compound can be measured if it can be trapped/retained by a denuder coating or filter paper, then extracted and quantitatively measured.

The objective of this research was to adapt the Chemcomb Speciation Sampling Cartridge to an REA system for the measurement of NH_3 fluxes in a high-NH_3 environment. First, the configuration of the system is discussed. Then the coating, handling, and capacity of the Chemcombs is described. Finally, preliminary field testing is presented.

3.2 Development of the REA Sampling System

3.2.1 System Configuration

The key to any REA system is designing a conditional air sampler that can independently collect up- and down-moving eddies. Typically, the REA sampling location is collocated above the surface adjacent to a sonic anemometer. A data acquisition and control system reads the anemometer and depending on the direction and magnitude of w, instantaneously activates valves that route gas samples into separate sample bags, denuders, or other types of chemical traps that receive either up eddies or down eddies. The design and function of the Chemcombs had to be carefully considered when adapting them to an REA system. Specifically, the Chemcombs were designed for

a constant, continuous flow rate. In addition, the Chemcombs needed to be located within the system in a way that would minimize the interaction of NH_3 with the system components (i.e., tubing walls, pump, etc.). To address these issues, a circulating airflow design was used (Figure 3.1). High-speed valves (091-0094-900, Parker Hannifin-General Valve, Fairfield, NJ) were attached to the inlets of the Chemcombs using PTFE tees (K-31320-35, Cole Parmer, Vernon Hills, IL) (Figure 3.2). The valves were activated based on w, as measured using a sonic anemometer (CSAT3, Campbell Scientific, Inc., Logan, UT). When an up-moving eddy was detected, the up valve was activated and air was pulled through the up-moving eddy Chemcomb, likewise when a down-moving eddy was detected, the down valve was activated and air was pulled through the down-moving eddy Chemcomb. If the magnitude of w was less than the deadband, neither valve was activated. Air was circulated through the Chemcombs with a dual head pump (R222-AT-AA1, Air Dimensions, Deerfield Beach, FL) and flowrates were controlled with mass flow controllers (0-15 L min^{-1}, AFCS36S-VADN5-C0A, Aalborg Instruments, Orangeburg, NY). Steel 0.5 – 1.0 L ballasts were located both upstream and downstream of the pump. The NH_3-free air exhausted from the pump (scrubbed by the Chemcombs) was routed back to the "common" ports of the high-speed valves. The "normally open" ports of the valves were attached to the Chemcomb inlets so that unless the valves were activated, NH_3-free air was continuously recirculated through the Chemcombs. When the valves were activated and air was sampled, the NH_3-free air was exhausted out the "normally closed" ports of the valves. Two pressure transducers with a range of 0 – 3.74 kPa (264, Setra, Boxbourough, MA) were attached to the exhaust ports of the valves with brass tees to remotely verify that the valves were functioning.

Mass flux could be calculated using an operational form of Equation 3.1 as follows:

$$\overline{F} = \beta \sigma_w \rho_d \left(\frac{m_u}{t f_u \alpha_u} - \frac{m_d}{t f_d \alpha_d} \right) \tag{3.2}$$

where F is the mass flux (mg m^{-2} s^{-1}), ρ_d is the dry air density (kg m^{-3}), m is the mass of NH_3 trapped in the up- or down-moving Chemcombs (mg), t is the total sample duration

(s), f is the continuous flowrate through the Chemcombs (kg dry air s^{-1}), and α is the fraction of time the up- or down-moving eddy valves are activated.

The Chemcomb inlets were positioned 24 cm from the sonic anemometer (Figure 3.2). An open-path infrared gas analyzer (LI-7500, Li-Cor Inc., Lincoln, NE) was positioned the same distance from the sonic anemometer and was used for the calculation of β via eddy covariance measurements of CO_2 and H_2O fluxes:

$$\beta = \frac{\overline{F}}{\rho\sigma_w\left(\overline{\chi^+} - \overline{\chi^-}\right)} \tag{3.3}$$

A CR5000 datalogger (Campbell Scientific, Inc.) was used for data collection and valve controls. Ancillary meteorological instrumentation included a relative humidity and temperature probe (HMP 45C, Campbell Scientific, Inc.), an infrared thermometer for surface temperature (4000.4ZL, Everest Interscience Inc., Tucson, AZ), a net radiometer (Q7.1, Campbell Scientific, Inc.), and a tipping bucket rain gauge (TE525, Campbell Scientific, Inc.). The REA system was positioned on a motorized tram attached to a trailer-mounted 10 m tower (Figure 3.2). The moveable tram allowed for easy servicing or reloading of the Chemcombs, and could quickly be positioned anywhere between 3 and 10 m.

The Chemcombs were designed for fairly high flow rates (i.e., 10 or 16.7 L min^{-1}). When the valves were in recirculating mode (i.e., not activated), the high flow rates caused a small amount of incursion of ambient air into the recirculating loop. To prevent this, supplemental NH_3-free air was injected into the recirculating loop so that there was a small amount of air flowing out of the sample inlet when the valves were not being activated. Lab testing was conducted to determine the minimum amount of supplemental air needed to prevent incursion at the inlet tip. An infrared gas analyzer (LI-6262, Li-Cor Inc.) was positioned in the recirculating loop, and pure CO_2 was blown across the inlet tip at various rates to simulate ambient wind. Based on historical sonic anemometer data taken from feedlots, the typical angle of attack of the ambient air at the sample tip was usually +/- 2 degrees, with a maximum of about 5 degrees, therefore a 10-degree angle of attack for the pure CO_2 was chosen as a worst case scenario. Results suggest that a maximum supplemental flow rate of 0.75 L min^{-1} limited incursion at the tip to negligible amounts (Figure 3.3). For example, with a 10 m s^{-1} simulated wind speed, a 10 degree

angle of attack, and a supplemental flow rate of 0.75 L min^{-1}, the rate increase in concentration was equivalent to about 30 mL of ambient air incursion over a 2-hour period, based on an internal system volume of 1.8 L. Thus, supplemental air was injected into the recirculating loop just before the high-speed valves, using N_2 tank gas controlled by two 0 –1.0 L min^{-1} mass flow controllers (MC-1LPM-D//5V, Alicat Scientific, Tucson, AZ). The flow rate of the supplemental air was between 0.25 and 0.75 L min^{-1}, and was adjusted every 30 min to be proportional to wind speed.

3.2.2 Chemcomb Handling

In order to measure NH_3 fluxes in the high NH_3 environment found at a feedlot, the Chemcombs had to be adapted for NH_3 only. The denuders were coated with a 1% w/w phosphoric acid in methanol solution, as recommended by Perrino and Gherardi (1999). The filterpack outlet held a 2.0 μm PTFE filter (P5PJ047, Pall Corporation, Ann Arbor, MI) followed by a cellulose filter (Whatman 41, Whatman Inc., Florham Park, NJ) coated with the same denuder coating solution. The manufacturer's recommended procedures for coating and extracting the denuders and filters were followed closely. The denuders were coated with the coating solution, dried with NH_3-free air, and capped until use. After deployment, NH_3 was extracted from the denuder walls with 10 mL of deionized water. Samples were then analyzed using ion chromatography (ICS-1000, Dionex Corporation, Sunnyvale, CA), including a cation-exchange analytical column (IonPac CS12A, 4 x 250 mm) and guard column (IonPac CG12A, 4 x 50 mm), a Cation Atlas Electolytic Suppressor, and 20mM methanesulfonic acid. One exception to the manufacturer's recommendions was that an NH_3-free bench for processing the denuders and loading the Chemcombs was deemed unnecessary after an analysis of blank denuders. Also, field testing revealed that extracted samples were sufficiently concentrated so that they could be analyzed colorimetrically via routine soil/water testing, rather than ion chromatography.

To determine the trapping capacity of the honeycomb denuders, an air stream of known NH_3 concentration (0.15 mg m^{-3}) was created using permeation tubes (Dynacal, VICI Metronics, Poulsbo, WA). This air stream was fed into the inlet of a Chemcomb and the output from the Chemcomb was monitored with a chemiluminescence NH_3

analyzer (17C, Thermo Scientific, Waltham, MA). The breakthrough of NH_3 with time for individual denuders and for 4 denuders in series is shown in Figure 3.4. The capacity of the honeycomb denuders was large, with the 4 denuders in series trapping over 1800 μg of NH_3 before breakthrough. In fact, field testing of the REA system showed that the short 2-denuder Chemcombs had more than enough capacity for 4-hour sample runs.

3.3 Field Testing

Field testing of the REA system was conducted at the Kansas State University Beef Research Center near Manhattan, KS. Fluxes were measured between 1000 and 1400 LST on eight days from July through September, 2007. The system was deployed along the north edge of a block of pens, taking advantage of the prevailing southerly wind direction (Figure 3.5). The sample area consisted predominantly of feedlot pens holding cattle weighing approximately 430 kg and stocked at a rate of about 15 m^2 $animal^{-1}$. The fringe of the sample area consisted mainly of densely stocked feeding barns and empty pens that were being cleaned. Meteorological conditions during the testing periods were warm and mostly sunny (Table 2.1).

Table 3.2 shows the analysis of the Chemcombs. The mass of NH_3 captured on the first denuder was always more than 90% of the total. Aerosol NH_4^+ trapped in the PTFE filter was negligible compared to the gaseous NH_3 trapped on the denuders. Amounts of NH_3 and NH_4^+ (collectively referred to as NH_x) captured by the backup cellulose filter were low, suggesting that the denuders were efficient. Average up-moving eddy concentrations were 580 μg m^{-3} and average down-moving eddy concentrations were 220 μg m^{-3}, for an average ambient air concentration of about 400 μg m^{-3} . When these concentrations were used to compute fluxes (Eq. 2), NH_3 emissions ranged between 60 and 130 μg m^{-2} s^{-1} (Table 3.3). The sampling time was almost equally split between the deadband ($.5\sigma_w$), the up-moving eddies, and the down-moving eddies. Calculated values of β were 0.41 – 0.45, similar to expected values. On September 21, four different 2-hour sample runs were conducted during a 24-hour period in order to look at the diurnal pattern of NH_3 fluxes. As expected, NH_3 fluxes exhibited the typical diurnal pattern, correlating well with latent heat fluxes (Figure 3.6).

3.4 Conclusions

Overall, the recirculating REA system worked better than expected. Two denuders in series had more than enough capacity for the 4-hour sample duration. Aerosol NH_4^+ was negligible compared to gaseous NH_3. Summer fluxes of NH_3 were from 60 – 130 μg m^{-2} s^{-1}, with concentration differences between the up- and down-moving eddies of 190 – 470 μg m^{-3}. Sample extracts from the denuders were concentrated enough that they could be analyzed with routine soil/water testing lab procedures. The diurnal pattern of NH_3 flux appears to correlate well with latent heat flux. This system was designed specifically for measuring NH_3 fluxes in high NH_3 environments, but could be applied to measure any compound that the denuders and/or filterpacks can be configured to capture.

References

ApSimon, H.M., Kruse, M., Bell, J.N.B., 1987. Ammonia emissions and their role in acid deposition. Atmos. Environ. 21, 1939-1946.

Beverland, I.J., ONeill, D.H., Scott, S.L., Moncrieff, J.B., 1996. Design, construction, and operation of flux measurement systems using the conditional sampling technique. Atmos. Env. 30(18), 3209-3220.

Bobbink, R., Hornung, M., Roelofs, J.G.M., 1998. The effects of air-borne nitrogen pollutants on species diversity in natural and semi-natural European vegetation. J. Ecol. 86, 717-738.

Bowling, D.R., Turnipseed, A.A., Delany, A.C., Baldocchi, D.D., Greenberg, J.P., Monson, R.K., 1998. The use of relaxed eddy accumulation to measure biosphere-atmosphere exchange of isoprene and other biological trace gases. Oecologia. 116, 306-315.

Brunet, J., Diekmann, M., Falkengren-Grerup, U., 1998. Effects of nitrogen deposition on field layer vegetation in south Swedish oak forests. Environ. Pollut. 102(SI), 35-40.

Businger, J.A., Oncley, S.P., 1990. Flux measurement with conditional sampling. J. Atmos. and Oceanic Tech. 7, 349-352.

Christensen, C.S., Hummelshoj, P., Jensen, N.O., Larsen, B., Lohse, C., Pilegaard, K., Skov, H., 2000. Determination of the terpene flux from orange species and Norway spruce by relaxed eddy accumulation. Atmos. Env. 34, 3057-3067.

Ferm, M., 1979. Method for determination of atmospheric ammonia. Atmos. Env. 13, 1385-1393.

Gaman, A., Rannik, U., Aalto, P., Pohja, T., Shvolo, E., Kulmala, M., Vesala, T., 2004. Relaxed eddy accumulation system for size-resolved aerosol particle flux measurements. J. Atmos. Oceanic Sci. 21, 933-943.

Guenther, A., Baugh, W., Davis, K., Hampton, G., Harley, P., Klinger, L., Vierling, L., Zimmerman, P., Allwine, E., Dilts, S., Lamb, B., Westberg, H., Baldocchi, D., Geron, C., Pierce, T., 1996. Isoprene fluxes measured by enclosure, relaxed eddy

accumulation, surface layer gradient, mixed layer gradient, and mixed layer mass balance techniques. J. Geophys. Res. 101(D13),18555-18567.

National Agricultural Statistics Service, United States Department of Agriculture. 2004. Cattle: final estimates 1999-2003. United States Government Printing Office. Washington D.C. http://usda.mannlib.cornell.edu/usda/nass/SB989/sb989.pdf

National Research Council. 2003. Air emissions from animal feeding operations: current knowledge, future needs. The National Academies Press. Washington D.C.

McInnes, K.J., Heilman, J.L., 2005. Relaxed eddy accumulation. Pp. 437-453. *In* M.K. Viney (ed.) Micrometeorology in Agricultural Systems. Agronomy Monograph no. 47. ASA-CSSA-SSSA, Madison, WI.

Perrino, C., Gherardi, M., 1999. Optimization of the coating layer for measurement of ammonia by diffusion denuders. Atmos. Env. 33, 4579-4587.

Pittcairn, C.E.R., Lieth, I.D., Sheppard, L.J., Sutton, M.A., Fowler, D., Munro, R.C., Tang, S., Wilson, D., 1998. The relationship between nitrogen deposition, species composition and foliar nitrogen concentrations in woodland flora in the vicinity of livestock farms. Environ. Pollut. 102(1/1), 41-48.

Shah, S.B., Westerman, P.W., Arogo, J., 2006. Measuring ammonia concentrations and emissions from agricultural land and liquid surfaces: a review. J. of Air and Waste Management Association. 56, 945-960.

Steinfeld, H., Gerber, P., Wassenaar, T., Castel, V., Rosales, M., de Haan, C., 2006. Livestock's Long Shadow: Environmental Issues and Options. Food and Agriculture Organization of the United Nations.

Sutton, M.A., Tang, Y.S., Miners, B., Fowler, D., 2001. A new diffusion denuder system for long-term, regional monitoring of atmospheric ammonia and ammonium. Water, Air, and Soil Pollution. Focus 1, 145-156.

United States Environmental Protection Agency. 2002. Consolidated emissions reporting; final rule. Fed. Register 67(111), 39602-39616.

Valentini, R., Greco, S., Seufert, G., Bertin, N., Ciccioli, P., Cecinato, A., Brancaleoni, E., Frattoni, M., 1997. Fluxes of biogenic VOC from Mediterranean vegetation by trap enrichment relaxed eddy accumulation. Atmos. Env. 31(SI), 229-238.

Zhu, T., Pattey, E., Desjardins, R.L., 2000. Relaxed eddy-accumulation technique for measuring ammonia volatilization. Environ. Sci. Technol. 34, 199-203.

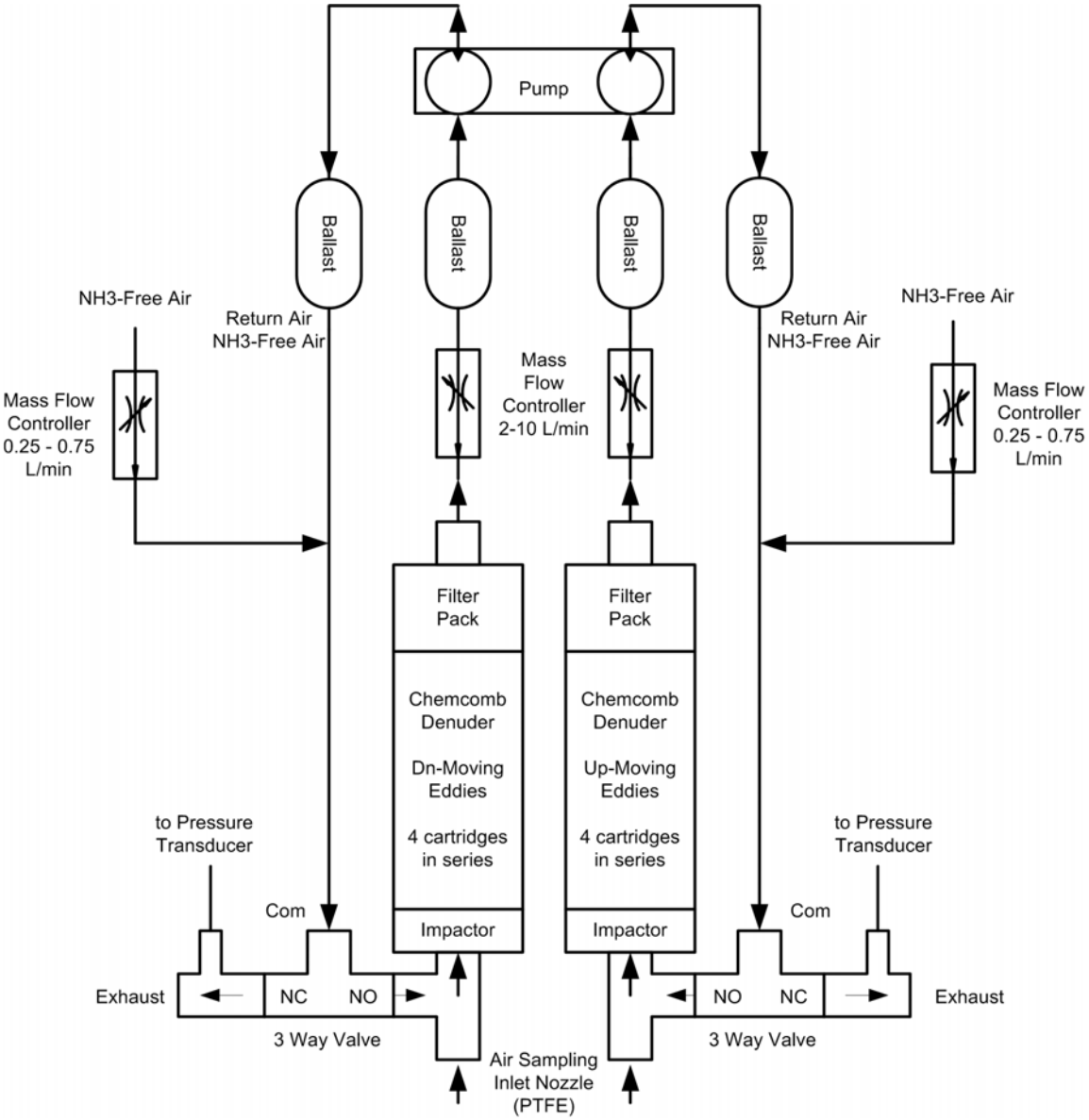

Figure 3.1 Diagram of the REA air sampling system.

Figure 3.2 (a) Photograph of the REA system assembled on a moveable tram that is lowered for servicing. (b) Close-up of the air inlet showing the valves, tees, and Chemcomb inlets.

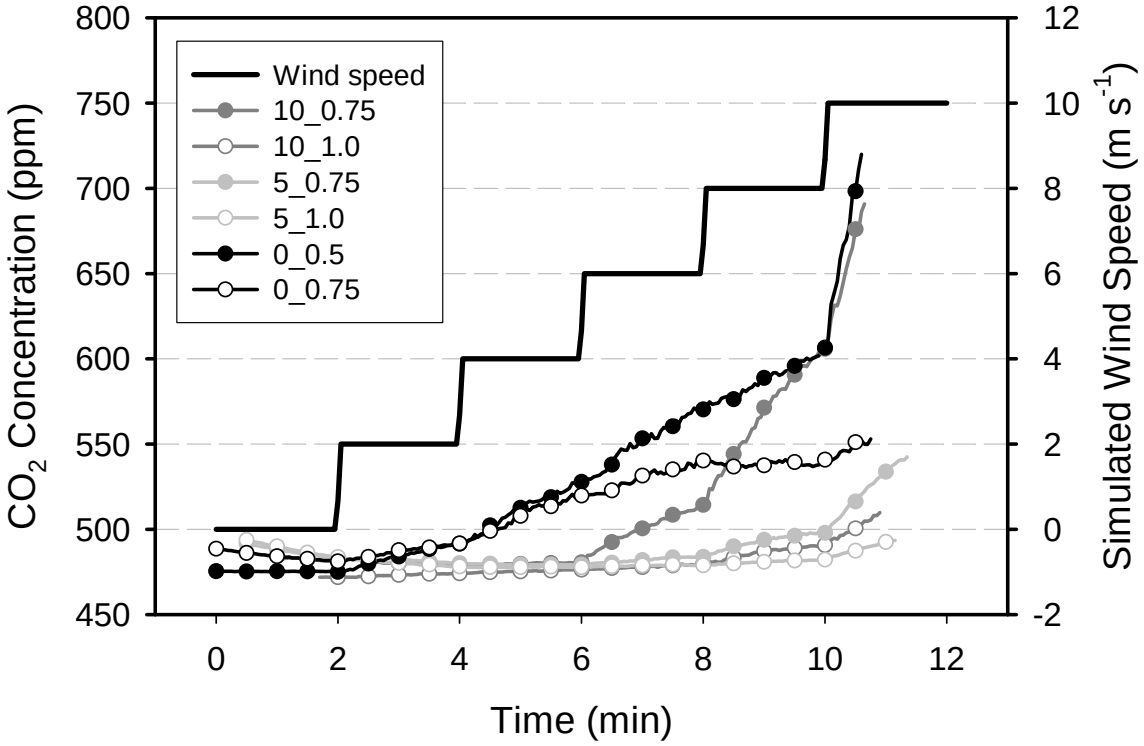

Figure 3.3 Rates of increase in CO_2 concentrations (left axis) within the recirculating loop, using various supplemental flow rates (L min^{-1}). Pure CO_2 was blown across the tip to simulate various wind speeds (right axis). In the legend, the numbers to the left of the underscore represent the angle of attack (degrees) and the numbers to the right represent the supplemental flowrate (L min^{-1}).

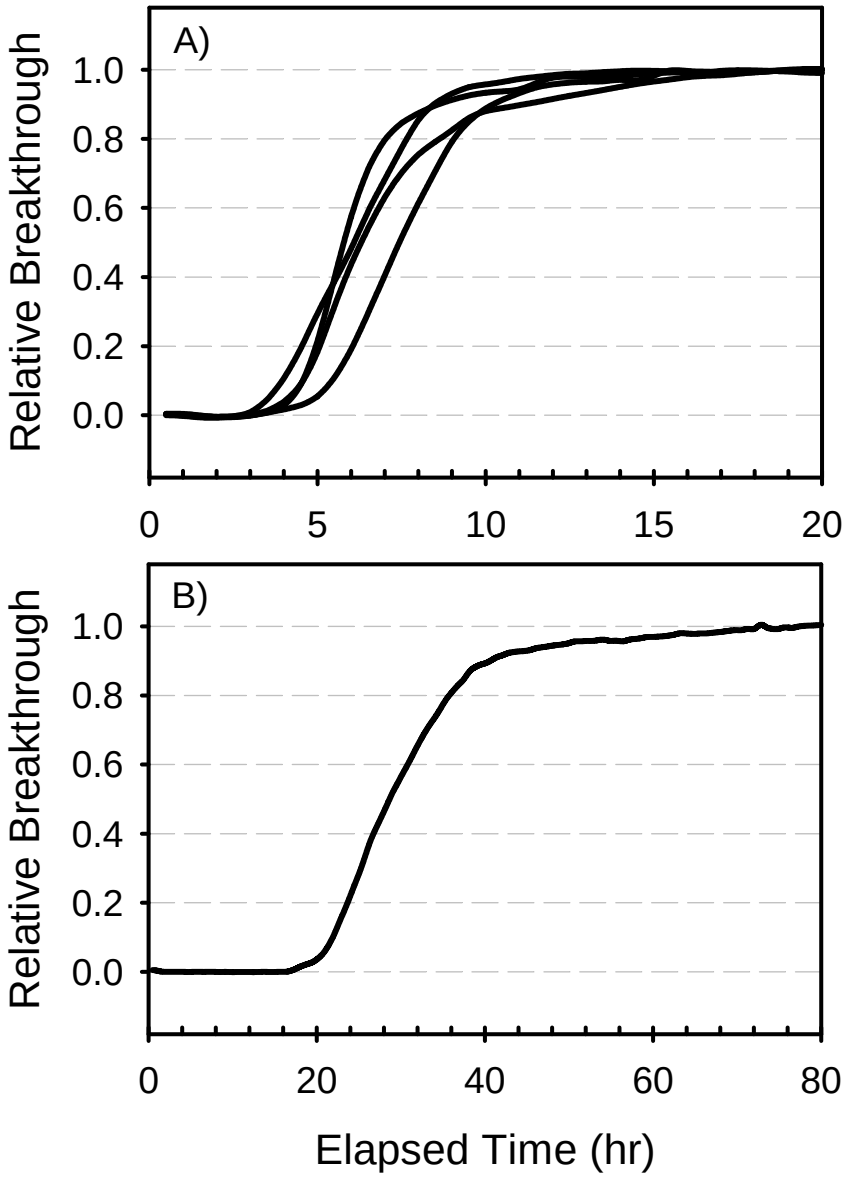

Figure 3.4 Relative breakthrough of NH_3 (i.e., concentration at the outlet divided by the concentration at the inlet) with time for (a) individual denuders and (b) four denuders in series.

Figure 3.5 Aerial map of the Kansas State University Beef Research Center near Manhattan, KS. The arrow near the top points to the location of the tower.

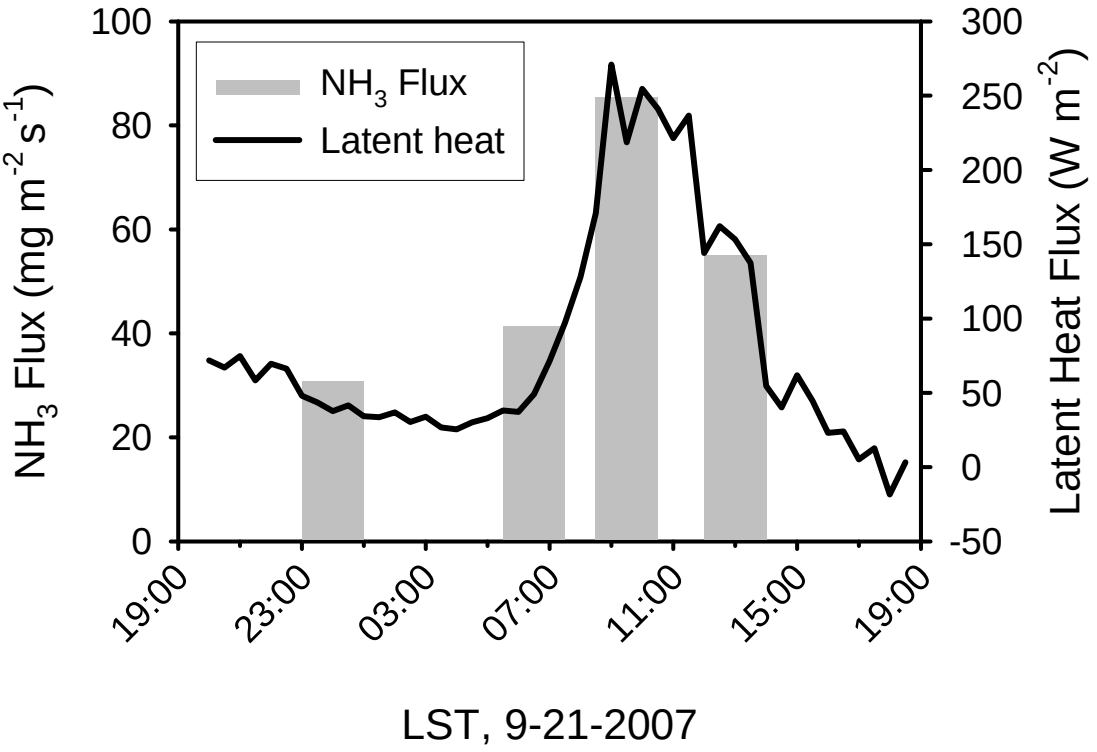

Figure 3.6 Measurements of NH_3 flux (left axis) taken over 2-hour sampling periods and the diurnal plot of latent heat flux (right axis).

Table 3.1 Average meteorological conditions during the sampling periods.

Day	Windspeed ($m\ s^{-1}$)	u* ($m\ s^{-1}$)	Air Temp. (C)	Surface Temp. (C)	Vapor Pressure (kPa)	Obukhov Length (m)
07/25	2.99	0.33	28.6	37.0	2.34	-29.6
07/26	2.82	0.33	30.9	42.4	2.11	-16.1
08/07	2.82	0.33	32.2	44.7	2.60	-15.9
08/08	4.21	0.50	32.0	45.1	2.71	-59.6
08/22	5.41	0.55	32.8	41.3	2.13	-65.7
08/23	4.90	0.51	31.8	39.2	2.08	-66.0
09/20	4.24	0.46	29.8	35.4	2.02	-117.7
09/24	5.00	0.51	29.0	34.2	1.67	-93.8
AVG	4.05	0.44	30.9	39.9	2.21	-58.1

Table 3.2 Chemcomb analysis and resulting NH_3 concentrations.

Day	Concentration ($\mu g\ NH_3\ m^{-3}$)		Denuder NH_3 mass (μg)		PTFE filter NH_4^+ mass (μg)		Cellulose backup filter NH_x mass (μg)	
	UP*	DN*	UP*	DN*	UP*	DN*	UP*	DN*
07/25	633.0	211.2	422.7	155.0	0.6	0.8	3.1	3.4
07/26	607.2	134.6	382.7	93.4	0.2	0.2	0.0	1.9
08/07	614.6	187.1	412.2	136.0	0.7	0.3	6.5	6.7
08/08	792.5	334.7	496.6	257.0	0.2	0.3	11.2	7.2
08/22	394.8	198.1	252.1	132.0	1.2	0.0	7.4	4.0
08/23	374.4	157.9	241.6	108.2	0.2	0.0	3.7	3.7
09/20	810.2	354.8	539.5	247.7	0.0	0.0	6.1	6.6
09/24	421.7	175.1	330.4	129.7	na**	na**	na**	na**
AVG	581.1	219.2	384.7	157.4	0.4	0.2	5.4	4.8

*"UP" and "DN" represent up-moving eddies and down-moving eddies, respectively.

**"na" represents data not available.

Table 3.3 Average measurements of NH_3, CO_2, latent heat, and sensible heat flux.

Day	σ_w ($m\ s^{-1}$)	deadband ($m\ s^{-1}$)	β	Concentration difference ($\mu g\ NH_3\ m^{-3}$)	NH_3 flux ($\mu g\ m^{-2}\ s^{-1}$)	CO_2 flux ($mg\ m^{-2}\ s^{-1}$)	Latent heat flux ($W\ m^{-2}$)	Sensible heat flux ($W\ m^{-2}$)
07/25	0.46	0.23	0.44	421.8	83.6	3.62	207.9	143.6
07/26	0.49	0.25	0.41	472.6	94.9	3.39	181.3	241.1
08/07	0.49	0.25	0.45	427.5	93.5	3.98	194.1	259.6
08/08	0.60	0.30	0.43	457.8	119.7	5.22	233.3	231.4
08/22	0.83	0.43	0.42	193.7	67.7	3.65	156.0	279.8
08/23	0.77	0.39	0.41	216.5	68.0	3.90	124.3	238.7
09/20	0.66	0.34	0.42	455.4	127.7	5.00	341.1	87.8
09/24	0.77	0.39	0.43	246.6	81.9	4.06	148.1	159.7
AVG	0.63	0.32	0.43	361.5	92.1	4.10	198.3	205.2

CHAPTER 4 - Conclusions

The first goal of this work was to assess the feasibility of using EC and other micrometeorological techniques for measuring emissions from a cattle feedlot. To accomplish this, we characterized the surface boundary layer of a commercial feedlot in western Kansas. Typically, this feedlot experienced high wind speeds and near-neutral atmospheric stability, so extrapolating from measurements made under calm and/or stable conditions is not advised as they would be very unrepresentative of typical conditions at feedlots in this region. Data showed a roughness length of 3.6 cm and a modeled displacement height of 65 cm. Thus, the surface is aerodynamically smooth as sensed from above, but one cannot ignore the contribution of the cattle (i.e., moving bluff bodies). Power spectra and cospectra showed the expected -2/3 and -4/3 slopes, respectively, in the inertial subrange, and there was no sign of turbulent features that would prohibit the use of EC or related techniques. In terms of daily emission rates per head, EC measurements of F_c and λE agreed with other studies measuring cattle respiration or water consumption. The percentage of the Hsieh modeled source area that represented actual fetch requirements for the feedlot was about 70% to 80%. Under neutral conditions, $X_{70\%}$ was about 360 m, representing a fetch to measurement height ratio of about 65:1. Even with a 6-m measuring height, the source area of the EC flux measurements was dominated by a small portion of the feedlot, with 61% of the signal originating from the three pens immediately south of the tower. Therefore, it would be especially important to know the characteristics of those pens when relating flux measurements back to nutrient loading, cattle diets, or stocking density. Finally, for researchers interested in flux measurements in terms of pen surface, the effects of non-pen surfaces on the measurements could be significant. Raw EC fluxes were typically increased by 11% to represent pen area fluxes but were sometimes scaled up by as much as 31%.

In summary, these guidelines should be followed when developing emission factors or making emissions measurements at cattle feedlots:

- Calm and/or stable atmospheric conditions are not typical at feedlots in the High Plains, so extrapolating from measurements made under these conditions is not advised.
- Even though the feedlot surface is aerodynamically smooth, as sensed at 6 m, one cannot ignore the contribution of the cattle as bluff rough elements, so flux measurements should not be made at heights less than 3 to 4 m.
- In general, fetch to measurement height ratios of 65:1 are adequate. Actual fetch requirements can be determined using an analytical footprint model (Hsieh et al., 2000) by calculating an upwind distance representing 70 to 80% of the modeled source area ($X_{70\%}$ - $X_{80\%}$).
- The source area of flux measurements is dominated by a very small portion of the feedlot, so in order to develop emission factors based on nutrient loading, cattle diets, stocking density, etc., it is particularly important to know the characteristics of the specific pens dominating the source area.
- When reporting flux measurements in terms of pen area, it is import to consider the effects of non-pen areas on the flux measurements, as they can be significant.

The second goal of this work was to develop a technology for measuring NH_3 emissions at cattle feedlots using REA. The objective was to adapt the Chemcomb Speciation Sampling Cartridge to a REA system for the measurement of NH_3 gases and NH_4^+ aerosol fluxes at cattle feedlots. This system utilized honeycomb denuders that independently sampled NH_3 in up-moving and down-moving eddies. Two denuders in series had more than enough capacity for the 4-hour sample duration. Aerosol NH_4^+ was negligible compared to gaseous NH_3. Summer fluxes of NH_3 were from 60 – 130 $\mu g\ m^{-2}\ s^{-1}$, with concentration differences between the up- and down-moving eddies of 190 – 470 $\mu g\ m^{-3}$. Sample extracts from the denuders were concentrated enough that they could be analyzed with routine soil/water testing lab procedures. This system was designed specifically for measuring NH_3 fluxes in high NH_3 environments, but could be applied to measure any compound that the denuders and/or filterpacks can be configured to capture.

Air emissions measurements from CAFOs are increasingly important, and indications are that micrometeorological techniques can be successfully applied to cattle feedlots in the High Plains. A new type of REA system was designed and fabricated for the measurement of NH_3 fluxes, and preliminary field testing showed that the system worked even better than expected. Future work should include more NH_3 emissions measurements at other feedlots using the new REA system. This system could potentially be adapted to measure acidic and basic gases in deposition studies. Results of this research provide a foundation for emissions measurements of NH_3 and other gases at cattle feedlots and help address some of the challenges that micrometeorologists face at feedlots. Additionally, this work has implications for emissions measurements from any heterogeneous, non-ideal surface.